ELSEVIER

Journal of Quantitative Spectroscopy & Radiative Transfer 107 (2007) 479–507

Journal of Quantitative Spectroscopy & Radiative Transfer

www.elsevier.com/locate/jqsrt

A successive order of scattering code for solving the vector equation of transfer in the earth's atmosphere with aerosols

J. Lenoble*,[1], M. Herman, J.L. Deuzé, B. Lafrance, R. Santer, D. Tanré

Laboratoire d'Optique Atmosphérique (LOA), Université des Sciences et Technologies de Lille, 59650 Villeneuve d'Ascq Cedex, France

Received 9 October 2006; received in revised form 14 March 2007; accepted 14 March 2007

Abstract

The paper presents in detail a code developed to solve the vector equation of radiative transfer. It is based on the successive orders of scattering and on the expansion into Fourier series of the azimuth; it includes the polarizing effects of aerosol scattering and of reflectance by water or terrestrial surfaces. The code is available from the authors upon request, and this detailed description aims at helping potential users to adapt the code to their own problem. Some examples of applications are given.

Keywords: Radiative transfer; Aerosols; Polarization; Successive scatterings

1. Introduction

In this paper, we present in some detail a radiative transfer (RT) code, developed over the years, at the Laboratoire d'Optique Atmosphérique (LOA) of Lille University. It includes a complete treatment of polarization due to aerosol scattering, and Earth's surface reflectance, and relies on the method of successive orders of scattering (OS); limited and simpler versions of the code are available and can be used.

The extraterrestrial solar radiation reaching the Earth's atmosphere is scattered by the air molecules and by the various solid and liquid particles (clouds, aerosols); it is also absorbed by gas molecules in several specific wavelength bands. The scattered radiation partly reaches the surface, and is partly reflected to space. In what follows we limit ourselves to the cloudless atmosphere, and outside the absorption bands with a line structure, as water vapor or carbon dioxide. Therefore we consider only scattering by air molecules and by aerosols; where necessary, we can easily include a continuum gas absorption like ozone absorption. We also assume the Earth's atmosphere to be plane-parallel, i.e. the characteristics vary only along the vertical direction.

The transfer of radiation inside the atmosphere is governed by the equation of transfer (ET), based on the conservation of energy, and allowing the calculation of radiance, and after angular integration, the calculation of irradiance; this so-called scalar ET remains very useful for many problems. However, as the scattering

*Corresponding author.
E-mail address: jacqueline.lenoble@ujf-grenoble.fr (J. Lenoble).
[1]Also at IRSA, Université Joseph Fourier, Grenoble, France.

0022-4073/$ - see front matter © 2007 Elsevier Ltd. All rights reserved.
doi:10.1016/j.jqsrt.2007.03.010

process modifies the state of polarization, the scalar ET is only approximate, and can lead to errors on the radiance reaching about 10% for a molecular atmosphere. Moreover the polarization of the scattered radiation contains in itself important information on the characteristics of the scattering particles, and it is used for improving aerosol remote sensing.

Numerous methods have been developed for solving the ET, both in the scalar and in the vector forms. A description of the methods, with a large list of references up to 1985, can be found in the collective book edited by Lenoble [1] under the auspices of the Radiation Commission of IAMAS. Since then, research has remained active, generally leading to numerical codes, and there are now several radiative transfer (RT) codes freely available to the users. Among the most popular, one can mention Libradtran [2], DISORT [3], TUV [4], Adding [5]; other RT models are presented in [6,7], and this list is far from being exhaustive. Most of these codes are big modular codes, tending to be as complete as possible and covering various kinds of problems, including longwave radiation. Even trying to be users' friendly, these big codes are not always easy to implement and some users take them as black boxes, without understanding how they operate. The recent research concerns mostly more complex problems. Important progress is presently made in designing 3-D codes necessary to handle real non uniform clouds [8]; other 3-D models are developed for twilight [9], and limb [10] observations.

Our code concerns the limited and somewhat simple probem of shortwave solar radiation in 1-D cloudless atmosphere. Its objective is analyzing radiation measurements, understanding the contribution of aerosol scattering and absorption, and of Earth's surface reflectance. The code allows the simultaneous introduction of several aerosol models with different characteristics and different profiles. It also offers the choice of different reflectance laws, for land and water surfaces.

The available modular codes are certainly very useful in some cases, however we did not find them a satisfactory solution to our own problems, and this was the first reason for starting this work. We believe that for many problems, at least the simple ones, it is much more efficient to write directly a code specifically designed for the problem considered. With a good knowledge of the radiative transfer theory, i.e. of the theoretical basis of the code, and only an elementary knowledge of a programming language, this is not a too demanding task. A variant of this approach is to use a code as ours, with the information included in this paper, in order to adapt the code to the user's specific problem. Our objective is not to provide the users' community with a new big code, competing with other codes already available, but to transmit our own experience in writing a RT code.

The code described here combines the expansion of the optical properties into generalized Legendre functions, with a Fourier expansion in the azimuth. This code is flexible and easy to use; it is available in different versions in FORTRAN, and it has been used successfully, by ourselves and by some other users for different problems.

In Section 2, we recall the theoretical basis of the code with the necessary definitions in Section 2.1; the polarization is most easily characterized by the four Stokes parameters defined in Section 2.2. The phase matrix, which characterizes the single scattering (including polarization) of the molecules and particles is presented in Section 2.3, with the necessary information on the aerosol phase matrix. Section 2.4 establishes the exact vector ET, to be used for obtaining the correct value of the radiance, as well as information on the polarization characteristics; the scalar ET is a special case of this vector ET. Section 3 is devoted to the method of successive orders of scattering (OS) and Section 4 presents the development of the ET and of the phase matrix into Fourier series, as it can be used in most of the ET solution methods. Section 5 adds the possibility of a reflecting lower boundary, as snow, water, or vegetation. According to our objective, we have tried to present the basis of the code as completely as possible, even if some points are classical and can be found elsewhere. The paper is therefore expected to be self-consistent. Finally, Section 6 presents some examples of applications of the OS codes developed at LOA for different problems, as remote sensing of aerosols and analysis of surface ultraviolet spectral irradiance; detailed results are not shown, as they are available in published papers; references are given. Conclusions are presented in Section 7.

2. Theoretical basis

In this section, we present the theoretical basis necessary for understanding our code; although most of these notions are classical, we think useful for the reader to have them summarized in a complete and consistent manner.

2.1. Definitions

As said previously, we consider a plane-parallel atmosphere, i.e. the only position coordinate of a point M is the altitude z above the surface. A direction $\mathbf{k}$ (see Figs. 1) is defined by the angle with the upward vertical, or zenith angle θ, between 0 and π, or preferably by the cosine of the zenith angle $\mu = \cos\theta$, and by an azimuth angle φ, counted from an arbitrary origin which is generally the sun meridian; φ is counted between 0 and 2π in the direct direction around Oz (i.e. in the clockwise direction when looking in the positive direction Oz; Fig. 1a). Let us note that $\mu > 0$ corresponds to upward directions and $\mu < 0$ to downward directions. The sun direction is $\mathbf{k}_0(\mu_0, \varphi_0)$, with μ_0 negative; if the sun meridian is used as origin, $\varphi_0 = 0$.

The local extinction of the radiance L, along a path $\mathrm{d}x$

$$\mathrm{d}L = -\sigma L\,\mathrm{d}x = -(\sigma_s + \sigma_a)L\,\mathrm{d}x \tag{1}$$

defines the local extinction coefficient σ, due to scattering (σ_s) and to absorption (σ_a). It is usual to introduce a single-scattering albedo (SSA) as

$$\omega = \sigma_s/\sigma. \tag{2}$$

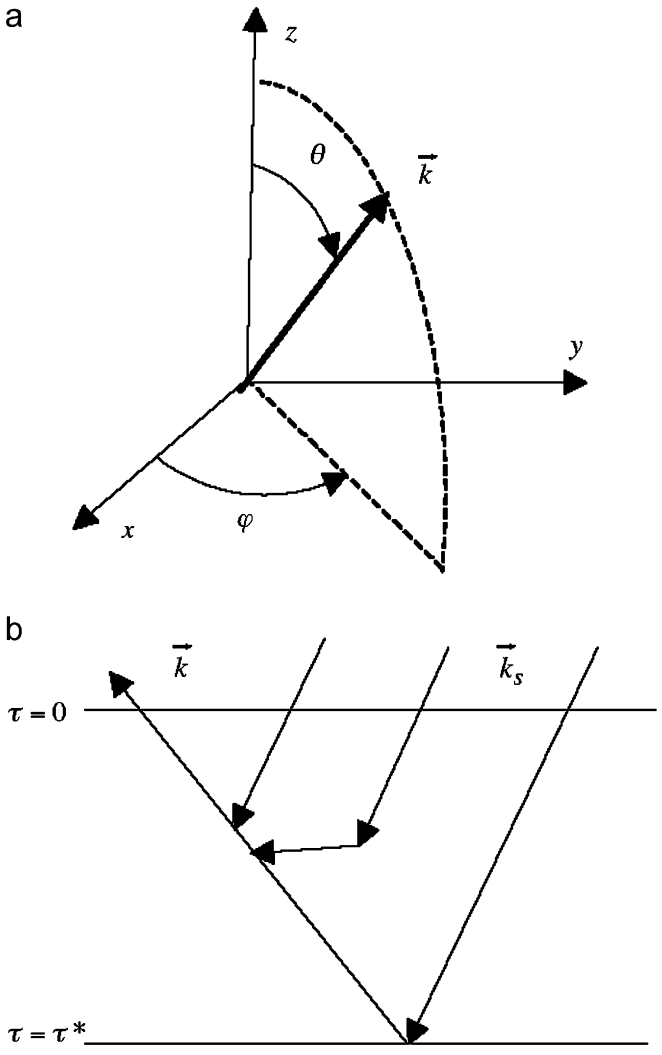

Fig. 1. (a) Characterization of the propagation direction, $\mathbf{k}$. (b) Optical depth, τ, and optical thickness, τ^*, of the atmosphere.

For a plane parallel atmosphere, the optical thickness of an element layer dz along the vertical is defined as

$$d\tau = -\sigma(z)dz. \tag{3}$$

The optical thickness τ measured from the top of the atmosphere to the level z, called optical depth (OD), is generally used instead of z as the altitude variable; τ increases downwards, which explains the minus sign in Eq. (3). The top of the atmosphere is at $\tau = 0$ and we will call τ^* the optical depth of the lower boundary, i.e. the total atmosphere optical thickness (Fig. 1b).

The phase function $p(\Theta)$ describes the probability of scattering as a function of the scattering angle Θ which is the angle between incident and scattered directions; $p(\Theta)$ is normalized to 4π when integrated over all directions.

The atmosphere is illuminated only with an irradiance — $\mu_0 E_0$ on its upper boundary by the solar beam in the direction (μ_0, φ_0). Inside the atmosphere the transmitted irradiance is

$$E_{tr}(\tau, \mu, \varphi) = \delta(\mu - \mu_0)\delta(\varphi - \varphi_0)E_0 e^{\tau/\mu_0}, \tag{4}$$

where $\delta(x)$ is the Dirac Delta function, equal to 1 for $x = 0$ and to 0 for x different from 0.

The diffuse radiative field is characterized by the radiance $L(M, \mathbf{k}) = L(\tau, \mu, \varphi)$. It is governed by the usual scalar equation of transfer that expresses the change of L along an element layer $d\tau$ crossed under the angle $\cos^{-1}\mu$, due to the loss of radiation by extinction, and to the gain by scattering from other directions.

A detailed derivation of the equation of transfer can be found in several textbooks (see [11–15]). In Section 2.4, we directly derive the vector ET and find the scalar ET as a particular case.

The radiance $L(\tau, \mu, \varphi)$ is obviously proportional to the incoming solar irradiance E_0. It also depends on the sun direction, and the variables (μ_0, φ_0) in the expression of L are omitted for simplicity. Moreover all atmospheric characteristics as well as the extraterrestrial solar radiation are wavelength dependent. The formalism used here concerns monochromatic radiation.

2.2. The Stokes parameters

Because the scattering process depends on the state of polarization, and modifies it, the radiance derived from the scalar ET is only an approximation which can differ from the exact value by errors of a few percent, even reaching 10% in the worst cases (see [16]). In this subsection, we present the Stokes parameters, which allow a convenient way to characterize the state of polarization of radiation.

An electromagnetic plane wave traveling in the direction $\mathbf{k}$ is characterized by the complex components E_l and E_r of its electric vector $\mathbf{E}$, on two orthogonal unitary axes $\mathbf{l}$ and $\mathbf{r}$ in the wave plane, or by any combination of the four parameters $E_l\hat{E}_l$, $E_r\hat{E}_r$, $E_r\hat{E}_l$, $E_l\hat{E}_r$, where $\hat{E}$ stands for the conjugate value of E. In this paper, the vectors $(\mathbf{l}, \mathbf{r}, \mathbf{k})$ constitute a right-handed Cartesian coordinate system (Fig. 2). The influence of chosing different conventions of sign is discussed in Appendix A.

The Stokes parameters (see [11,17]) are defined as

$$\begin{pmatrix} I \\ Q \\ U \\ V \end{pmatrix} = \frac{\varepsilon_0 c}{2}\begin{pmatrix} \langle E_l\hat{E}_l\rangle + \langle E_r\hat{E}_r\rangle \\ \langle E_l\hat{E}_l\rangle - \langle E_r\hat{E}_r\rangle \\ \langle E_l\hat{E}_r\rangle + \langle E_r\hat{E}_l\rangle \\ i\langle E_l\hat{E}_r\rangle - i\langle E_r\hat{E}_l\rangle \end{pmatrix} = \frac{\varepsilon_0 c}{2}\begin{pmatrix} \langle E_{l0}^2\rangle + \langle E_{r0}^2\rangle \\ \langle E_{l0}^2\rangle - \langle E_{r0}^2\rangle \\ \langle 2E_{l0}E_{r0}\cos\delta\rangle \\ \langle 2E_{l0}E_{r0}\sin\delta\rangle \end{pmatrix}, \tag{5}$$

where E_{l0} and E_{r0} are the amplitudes of E_l and E_r, respectively, and δ is the retardation in phase of E_l relative to the phase of E_r; c is the velocity of light in the vacuum, and ε_0 the dielectric constant in vacuum. As measurements always include a large number of wave trains, the quantities $\langle x\rangle$ are the temporal averages of x. These average Stokes parameters contain all the available information on the radiation field (see [11]). I is the total radiative energy, i.e. it is identical to the irradiance E, or to the radiance L, considered in the previous section. The three other parameters have the same dimensions as I ($W\,m^{-2}$ or $W\,m^{-2}\,sr^{-1}$); they serve to characterize the state of polarization, as explained below.

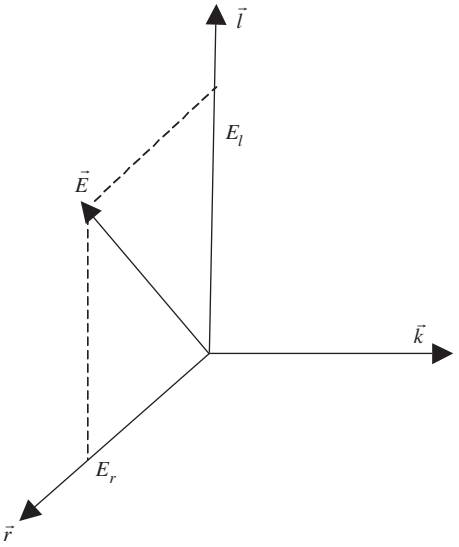

Fig. 2. The $(\mathbf{r}, \mathbf{l}, \mathbf{k})$ coordinate system.

The state of polarization is determined by δ and by the ratio $a = E_{l0}/E_{r0}$. For a mixture of incoherent wave trains, with the same average amplitudes, $Q = U = V = 0$, the radiation is natural or non-polarized. This is the case of the extraterrestrial solar radiation.

When several independent streams of radiation are combined, the Stokes parameters of the mixture are the sums of the Stokes parameters of the components; the axes **l** and **r** have to be the same for all the added components. Due to the additivity of the Stokes parameters, any beam can be analyzed as the incoherent superposition of polarized radiation with an intensity

$$I_{\text{pol}} = (Q^2 + U^2 + V^2)^{1/2} \tag{6}$$

and natural radiation; the degree of polarization is

$$P = I_{\text{pol}}/I. \tag{7}$$

For linear polarization, $\delta = 0$ and $V = 0$, and the two parameters Q and U fix the direction of polarization. If α is the angle of rotation around **k** which brings **l** parallel to **E**, with α counted positive in the direct direction around **k** (Fig. 3)

$$\begin{aligned} Q &= I_{\text{pol}} \cos(2\alpha), \\ U &= I_{\text{pol}} \sin(2\alpha). \end{aligned} \tag{8}$$

For elliptically polarized light, the parameter V defines the ellipticity of the polarized light; V is generally very small in the atmosphere and it is often neglected, the polarization being considered as linear.

The usual scalar quantities, as radiance or irradiance, are conveniently replaced by a radiance (or irradiance) vector, built of the Stokes parameters,

$$\mathbf{L} = (I, Q, U, V)^{\text{T}} \tag{9}$$

where $\mathbf{x}^{\text{T}}$ means the transpose of vector **x**.

2.3. The phase matrix

In order to describe the effect of scattering on polarization, the scalar phase function $p(\Theta)$ has to be replaced by a 4×4 phase matrix.

Let us choose reference axes $(\mathbf{l}', \mathbf{r}')$ and $(\mathbf{l}, \mathbf{r})$, for the incident and scattered radiation parallel and perpendicular to the scattering plane, defined by the directions of incidence and of scattering. For a

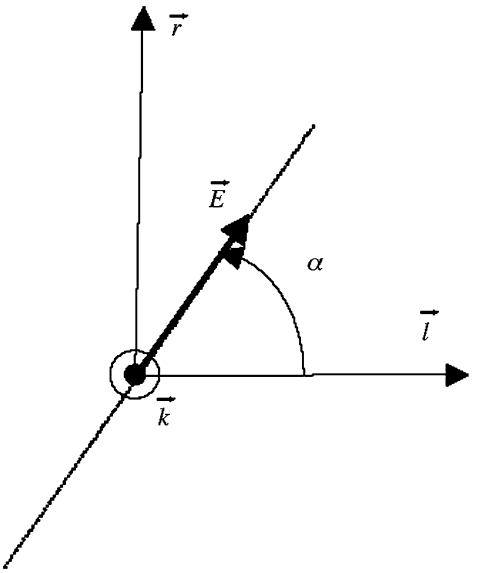

Fig. 3. Description of linearly polarized light.

distribution of randomly oriented particles, in equal number with their miror particles (see [18]), which is not a very restrictive condition for aerosols, the phase matrix is in the form

$$\mathbf{P}(\Theta)=\begin{pmatrix} P_{11}(\Theta) & P_{12}(\Theta) & 0 & 0 \\ P_{21}(\Theta) & P_{22}(\Theta) & 0 & 0 \\ 0 & 0 & P_{33}(\Theta) & P_{34}(\Theta) \\ 0 & 0 & P_{43}(\Theta) & P_{44}(\Theta) \end{pmatrix}. \tag{10}$$

The upper left element $P_{11}(\Theta)$ is identical to the phase function $p(\Theta)$. The four upper right and the four lower left elements are zero, and $P_{21}=P_{12,}\ P_{43}=-P_{34}$; only six elements are needed. For spherical particles, further simplifications occur, $P_{22}=P_{11,}\ P_{44}=P_{33,}$ and only four elements are necessary. The phase matrix is obtained from the Mie theory [19]. For molecular scattering by anisotropic molecules, the phase matrix is given in Refs. [11,20]; P_{34} and P_{43} are zero but $P_{22}\neq P_{11,}P_{44}\neq P_{33,}$ and four elements also are necessary. The problem is more difficult for non-spherical particles, but the phase matrix has been obtained for various shapes, mostly by the T-matrix code by Mishchenko et al. [21] for small aerosol particles. The phase matrix has also been measured in the laboratory, for different particles by Volten et al. [22].

It is usual to develop the phase function into a series of Legendre polynomials $P_l(\cos\Theta)$

$$p(\Theta)=\sum\nolimits_{l=0}^{L}\beta_l P_l(\cos\,\Theta), \tag{11}$$

where the normalization of the phase function imposes $\beta_0=1$. The order L of the development depends on the scattering particles (see Section 6). The usefulness of this expansion will appear in Section 4 when developing into Fourier series. With the same objective (see [23–25]), it is useful to expand the six elements of the phase matrix into the form

$$P_{11}(\Theta)=p(\Theta)=\sum_{l=0}^{L}\beta_l P_l(\cos\,\Theta),$$

$$P_{21}(\Theta)=P_{12}(\Theta)=\sum_{l=2}^{L}\gamma_l P_2^l(\cos\,\Theta),$$

$$P_{22}(\Theta) = \sum_{l=2}^{L} [\alpha_l R_2^l(\cos\Theta) + \varsigma_l T_2^l(\cos\Theta)],$$

$$P_{33}(\Theta) = \sum_{l=2}^{L} [\varsigma_l R_2^l(\cos\Theta) + \alpha_l T_2^l(\cos\Theta)],$$

$$P_{43}(\Theta) = -P_{34}(\Theta) = \sum_{l=2}^{L} \varepsilon_l P_2^l(\cos\Theta),$$

$$P_{44}(\Theta) = \sum_{l=0}^{L} \delta_l P_l(\cos\Theta), \tag{12}$$

where

$$R_s^l(\cos\Theta) = [P_{s,2}^l(\cos\Theta) + P_{s,-2}^l(\cos\Theta)]/2, \tag{13a}$$

$$T_s^l(\cos\Theta) = [P_{s,2}^l(\cos\Theta) - P_{s,-2}^l(\cos\Theta)]/2. \tag{13b}$$

The functions $P_{m,n}^l(\Theta)$ are generalized Legendre functions, introduced by Gel'fand and Sapiro [26] (see Appendix B), which reduce for $m = n = 0$, to the usual Legendre polynomial $P_l(\mu)$, and for $n = 0$, to the associated Legendre functions $P_m{}^l(\mu)$. For Rayleigh scattering by anisotropic molecules, $L = 2$ with

$$\begin{aligned} &\beta_0 = 1, \beta_1 = 0, \quad \beta_2 = x/2, \\ &\delta_0 = 0, \delta_1 = 3y/2, \\ &\gamma_2 = -(3/2)^{1/2} x, \quad \alpha_2 = 3x, \varepsilon_2 = \varsigma_2 = 0. \end{aligned} \tag{14}$$

In Eq. (14), $x = 2(1-\delta)/(2+\delta)$, $y = 2(1-3\delta)/(2+\delta)$ where δ is the molecular depolarization factor [20].

2.4. The vector equation of transfer

Because the Stokes parameters, as the scalar radiance, are additive when several streams of radiation are superposed, a vector equation governing the radiance vector $\mathbf{L}(\tau, \mu, \varphi)$ defined by Eq. (9) can be established in the same way as the scalar equation of transfer. The condition is that all the Stokes parameters added are refered to the same directions $\mathbf{l}$ and $\mathbf{r}$; the obvious choice is to take $\mathbf{l}$ and $\mathbf{r}$, respectively parallel and perpendicular to the vertical plane containing $\mathbf{k}$. When incident radiation from the direction (μ', φ') is scattered into a direction (μ, φ), because the scattering matrix is defined with axes parallel and perpendicular to the scattering plane, it is necessary to perform a double-axis rotation. First the axes $(\mathbf{l}', \mathbf{r}')$ associated to the incidence direction are rotated around $\mathbf{k}'$ by an angle χ' (see Fig. 4), to bring them parallel and perpendicular to the scattering plane. With χ' counted positive in the direct direction around $\mathbf{k}'$, this rotation corresponds to a multiplication of the radiance matrix by a transformation matrix

$$\mathbf{T}(\chi') = \begin{pmatrix} 1 & 0 & 0 & 0 \\ 0 & \cos(2\chi') & \sin(2\chi') & 0 \\ 0 & -\sin(2\chi') & \cos(2\chi') & 0 \\ 0 & 0 & 0 & 1 \end{pmatrix}. \tag{15}$$

After application of the phase matrix $\mathbf{P}(\Theta)$ for the angle Θ between the directions (μ', φ') and (μ, φ), a second rotation of $-\chi$ is performed, in order to have the scattered radiance matrix refered to $(\mathbf{l}, \mathbf{r})$ (Fig. 4).

The vector ET writes as

$$\mu \frac{d\mathbf{L}(\tau, \mu, \varphi)}{d\tau} = \mathbf{L}(\tau, \mu, \varphi) - \mathbf{S}(\tau, \mu, \varphi) \tag{16a}$$

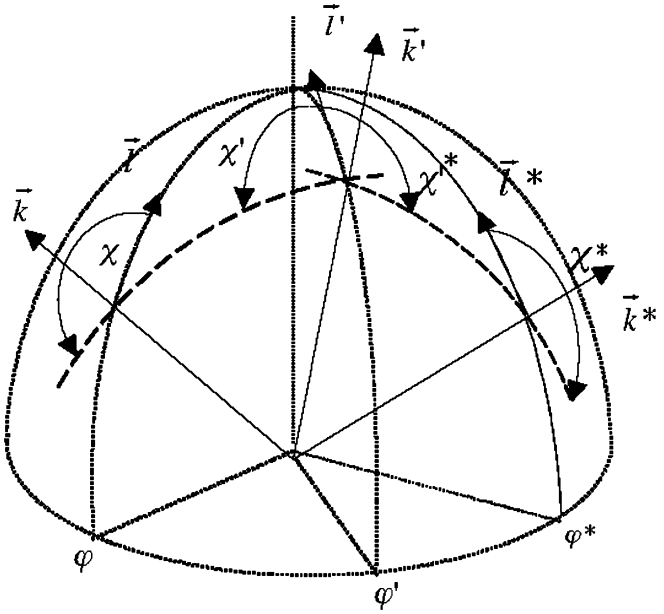

Fig. 4. Definition of the rotation angles, χ and χ'. Scattering directions (θ, φ) and (θ^*, φ^*), symmetric about the vertical plane which contains the incident direction (θ', φ'), correspond to opposite rotation angles, (χ, χ') and (χ^*, χ'^*), respectively.

with a source matrix

$$\mathbf{S}(\tau,\mu,\varphi)=\frac{\omega(\tau)}{4\pi}\,\mathbf{P}(\tau,\mu,\varphi,\mu_0,\varphi_0)\mathbf{E}_0\exp(\tau/\mu_0)+\frac{\omega(\tau)}{4\pi}\int_0^{2\pi}\int_{-1}^{+1}\mathbf{P}(\tau,\mu,\varphi,\mu',\varphi')\mathbf{L}(\tau,\mu',\varphi')\,\mathrm{d}\mu'\,\mathrm{d}\varphi'. \tag{16b}$$

The first term on the right-hand side corresponds to single scattering of the direct solar beam, and the second term to multiple scatterings. As said before, we do not consider thermal emission in the source function. As explained above, the kernel 4×4 matrix $\mathbf{P}$ in Eq. (16b) is

$$\mathbf{P}(\tau,\mu,\varphi,\mu',\varphi')=\mathbf{T}(-\chi)\mathbf{P}(\tau,\Theta)\mathbf{T}(\chi') \tag{17}$$

and the irradiance matrix for the incident non-polarized solar radiation is

$$\mathbf{E}_0=(E_0,0,0,0)^{\mathrm{T}}. \tag{18}$$

Integrating Eq. (16a) leads to

$$\mathbf{L}(\tau,\mu<0,\varphi)=-\int_0^{\tau}e^{-(\tau'-\tau)/\mu}\mathbf{S}(\tau',\mu,\varphi)\,\mathrm{d}\tau'/\mu, \tag{19a}$$

$$\mathbf{L}(\tau,\mu>0,\varphi)=\mathbf{L}^{\mathrm{up}}(\tau^*,\mu>0,\varphi)e^{-(\tau^*-\tau)/\mu}+\int_{\tau}^{\tau^*}e^{-(\tau'-\tau)/\mu}\mathbf{S}(\tau',\mu,\varphi)\,\mathrm{d}\tau'/\mu \tag{19b}$$

with no diffuse radiation incident on the top of the atmosphere; $\mathbf{L}^{\mathrm{up}}$ depends on the surface reflectance, as discussed in Section 5. It is zero for a black ground. Eqs. (19) are the form of the ET that the successive orders of scattering work with.

The vector equations are equivalent to four coupled equations for the Stokes parameters I, Q, U, V of the radiance $\mathbf{L}$. The scalar ET is simply the first of these equations written for $L=I$, with $Q=U=V=0$, and $P_{11}=p$, the phase function, accounting for the form of $\mathbf{T}$.

3. The method of successive orders of scattering

The idea underlying the method of successive orders of scattering, is to separate the radiance into the contributions of photons scattered once, twice, …, n times

$$\mathbf{L}(\tau,\mu,\varphi)=\sum_{n=1}^{N}\mathbf{L}_n(\tau,\mu,\varphi). \tag{20}$$

It has been suggested very early, first limited to two terms by Hammad and Chapman [27], used by several authors in somewhat different forms, and recently by Min and Duan [28]; a rather large bibliography can be found in [1].

Starting from Eqs. (19), it leads obviously to

$$\mathbf{L}_n(\tau,\mu<0,\varphi)=-\int_0^{\tau}e^{-(\tau'-\tau)/\mu}\mathbf{S}_n(\tau',\mu,\varphi)\,\mathrm{d}\tau'/\mu, \tag{21a}$$

$$\mathbf{L}_n(\tau,\mu>0,\varphi)=\mathbf{L}_n^{\mathrm{up}}(\tau^*,\mu>0,\varphi)e^{-(\tau^*-\tau)/\mu}+\int_{\tau}^{\tau^*}e^{-(\tau'-\tau)/\mu}\mathbf{S}_n(\tau',\mu,\varphi)\,\mathrm{d}\tau'/\mu, \tag{21b}$$

where

$$\mathbf{S}_1(\tau,\mu,\varphi)=\frac{\omega(\tau)}{4\pi}\mathbf{P}(\tau,\mu,\varphi,\mu_0,\varphi_0)\mathbf{E}_0e^{\tau/\mu_0}, \tag{21c}$$

$$\mathbf{S}_{n>1}(\tau,\mu,\varphi)=\frac{\omega(\tau)}{4\pi}\int_0^{2\pi}\int_{-1}^{+1}\mathbf{P}(\tau,\mu,\varphi,\mu',\varphi')\mathbf{L}_{n-1}(\tau,\mu',\varphi')\,\mathrm{d}\mu'\,\mathrm{d}\varphi' \tag{21d}$$

and considering that one reflection is similar to one scattering,

$$\mathbf{L}_1^{\mathrm{up}}(\tau^*,\mu>0,\varphi)=(-\mu_0)\mathbf{R}(\mu,\varphi,\mu_0,\varphi_0)\mathbf{E}_0e^{\tau^*/\mu_0}/\pi, \tag{21e}$$

$$\mathbf{L}_{n>1}^{\mathrm{up}}(\tau^*,\mu>0,\varphi)=\int_0^{2\pi}\int_{-1}^{0}(-\mu')\mathbf{R}(\mu,\varphi,\mu',\varphi')\mathbf{L}_{n-1}(\tau^*,\mu',\varphi')\,\mathrm{d}\mu'\,\mathrm{d}\varphi'/\pi. \tag{21f}$$

Equation (21e) defines the reflectance matrix of the surface $\mathbf{R}(\mu,\varphi,\mu_0,\varphi_0)$, as a generalization of the simple Lambertian reflectance ρ, which leads for L^{up} to $(-\mu_0)\rho\mathbf{E}_0e^{\tau*/\mu_0}/\pi$, in Eq. (21e). Note that, in Eqs. (21c) and (21e), e^{τ/μ_0} is the transmittance of the direct solar beam in a plane parallel atmosphere. The direct transmittance, $T_{\mathrm{sph}}(\tau,\mu_0)$, taking into account the Earth's sphericity, can easily be computed and used instead of e^{τ/μ_0}, which leads to the so-called pseudo spherical code.

4. Expansion into Fourier series of azimuth

Expanding the various quantities into Fourier series of the azimuth allows us a separation of the variables μ and φ, which strongly simplifies the resolution of the ET.

For the scalar problem, the radiance is symmetric about the vertical plane containing the solar incident beam (μ_0, φ_0) and the phase function is symmetric about the vertical plane containing the incident direction (μ', φ'); therefore we can write

$$L(\tau,\mu,\varphi)=\sum_{s=0}^{S}(2-\delta_{0s})\cos(s(\varphi-\varphi_0))L^s(\tau,\mu), \tag{22}$$

$$p(\tau,\mu,\varphi,\mu',\varphi')=\sum_{s=0}^{S}(2-\delta_{0s})\cos(s(\varphi-\varphi'))p^s(\tau,\mu,\mu'), \tag{23}$$

where δ_{0s} ($=1$ for $s=0$, $=0$ otherwise) is introduced for commodity. In Eq. (22), the order S of the development is clearly limited to L in Eq. (11). The useful numerical value for S is discussed in Section 6.

Using the development of the phase function into series of Legendre polynomials and the additivity theorem of these polynomials (see Appendix B), it is easy to find the expression of $p^s(\mu,\mu')$. After integration over φ' of the source function, one easily gets the classical separation in azimuth of the scalar ET.

Generalization to the vector case has been examined by several authors (see [23–25]), and we just recall the main lines of the development.

We restrict to scattering and reflectance laws with axial symmetry, i.e. with $\mathbf{P}(\tau,\mu,\varphi,\mu',\varphi')$ and $\mathbf{R}(\mu,\varphi,\mu',\varphi')$ in the form $\mathbf{P}(\tau,\mu,\mu',\varphi-\varphi')$ and $\mathbf{R}(\mu,\mu',\varphi-\varphi')$, so that the radiance field is symmetric about the solar incident plane with

$$\begin{aligned}
I_n(\tau,\mu,\varphi) &= \sum_{s=0}^{S}(2-\delta_{0s})\cos(s(\varphi-\varphi_0))I_n^s(\tau,\mu),\\
Q_n(\tau,\mu,\varphi) &= \sum_{s=0}^{S}(2-\delta_{0s})\cos(s(\varphi-\varphi_0))Q_n^s(\tau,\mu),\\
U_n(\tau,\mu,\varphi) &= \sum_{s=1}^{S}2\,\sin(s(\varphi-\varphi_0))U_n^s(\tau,\mu),\\
V_n(\tau,\mu,\varphi) &= \sum_{s=1}^{S}2\,\sin(s(\varphi-\varphi_0))V_n^s(\tau,\mu),
\end{aligned} \tag{24}$$

i.e.

$$\mathbf{L}_n(\tau,\mu,,\varphi) = \sum_{s=0}^{S}(2-\delta_{0s})[\cos(s(\varphi-\varphi_o))\mathbf{L}^s_{n,\cos}(\tau,\mu)+\sin(s(\varphi-\varphi_0))\mathbf{L}^s_{n,\sin}(\tau,\mu)] \tag{25}$$

with

$$\mathbf{L}^s_{n,\cos}(\tau,\mu) = (I_n^s, Q_n^s, 0, 0)^{\mathrm{T}} \text{ and } \mathbf{L}^s_{n,\sin}(\tau,\mu) = (0, 0, U_n^s, V_n^s)^{\mathrm{T}}. \tag{26}$$

The parity of U and V corresponds to polarized vibrations with opposite inclinations and opposite turning directions when refered to the (**l,r,k**) axes on either side of the incident plane.

Given the matrix multiplication in Eq. (17), $\mathbf{P}(\mu,\varphi,\mu',\varphi')$ is in the form

$$\mathbf{P}(\mu,\varphi,\mu',\varphi') = \begin{pmatrix} P_{11} & c'P_{12} & s'P_{12} & 0\\ cP_{12} & cc'P_{22}+ss'P_{33} & cs'P_{22}-sc'P_{33} & sP_{43}\\ sP_{12} & sc'P_{22}-cs'P_{33} & ss'P_{22}+cc'P_{33} & -cP_{43}\\ 0 & -s'P_{43} & c'P_{43} & P_{44}\end{pmatrix}, \tag{27}$$

where the $P_{ij}(\Theta)$ are the coefficients of the phase matrix, Eq (10), and c stands for $\cos(2\chi)$, s for $\sin(2\chi)$, and similarly for c' and s' with χ'. The variable τ has been omitted.

Since scattering directions symmetric about the incident plane correspond to similar values for the $P_{ij}(\Theta)$ elements but opposite numerical values for χ and χ' (see Fig. 4), $\mathbf{P}(\mu,\varphi,\mu',\varphi')$ clearly separates into a symmetric and an anti-symmetric matrices with respect to $(\varphi-\varphi')$, which may be expanded, respectively, into series of $\cos(s(\varphi-\varphi'))$ and $\sin(s(\varphi-\varphi'))$, and

$$\mathbf{P}(\mu,\varphi,\mu',\varphi') = \sum_{s=0}^{L}(2-\delta_{0s})[\cos[s(\varphi-\varphi')]\mathbf{P}^s_{\cos}(\mu,\mu')+\sin[s(\varphi-\varphi')]\mathbf{P}^s_{\sin}(\mu,\mu')] \tag{28}$$

with

$$\begin{pmatrix} P_{11} & c'P_{12} & 0 & 0\\ cP_{12} & cc'P_{22}+ss'P_{33} & 0 & 0\\ 0 & 0 & ss'P_{22}+cc'P_{33} & -cP_{43}\\ 0 & 0 & c'P_{43} & P_{44}\end{pmatrix} = \sum_{s=0}^{L}(2-\delta_{0s})\cos[s(\varphi-\varphi')]\mathbf{P}^s_{\cos}(\mu,\mu'), \tag{29a}$$

$$\begin{pmatrix} 0 & 0 & s'P_{12} & 0 \\ 0 & 0 & cs'P_{22} - sc'P_{33} & sP_{43} \\ sP_{12} & sc'P_{22} - cs'P_{33} & 0 & 0 \\ 0 & -s'P_{43} & 0 & 0 \end{pmatrix} = \sum_{s=1}^{L} 2\,\sin[s(\varphi - \varphi')]\mathbf{P}^s_{\sin}(\mu, \mu'). \tag{29b}$$

Inserting Eqs. (25) and (28) in Eqs. (21c) and (21d) and integrating over φ' leads immediately to the development of the source function into Fourier series, with

$$\mathbf{S}_1(\tau, \mu, \varphi) = \frac{\omega(\tau)}{4\pi} \sum_{s=0}^{S} (2 - \delta_{0s}) \cos[s(\varphi - \varphi_0)]\mathbf{P}^s_{\cos}(\mu, \mu_0)\mathbf{E}_0 e^{\tau/\mu_0}, \tag{30a}$$

$$\begin{aligned} \mathbf{S}_{n>1}(\tau, \mu, \varphi) = \frac{\omega(\tau)}{2} \sum_{s=0}^{S} (2 - \delta_{0s}) \Bigg[& \cos[s(\varphi - \varphi_o)] \int_{-1}^{+1} (\mathbf{P}^s_{\cos}\mathbf{L}^s_{n-1,\cos} - \mathbf{P}^s_{\sin}\mathbf{L}^s_{n-1,\sin})\, \mathrm{d}\mu' \\ & + \sin[s(\varphi - \varphi_o)] \int_{-1}^{+1} (\mathbf{P}^s_{\sin}\mathbf{L}^s_{n-1,\cos} + \mathbf{P}^s_{\cos}\mathbf{L}^s_{n-1,\sin})\, \mathrm{d}\mu' \Bigg]. \end{aligned} \tag{30b}$$

The variables τ, μ, μ' have been omitted in the integral terms. The problem is to derive the coefficients of the matrices $\mathbf{P}^s_{\cos}(\mu, \mu')$ and $\mathbf{P}^s_{\sin}(\mu, \mu')$. The hint was firstly suggested by Kuscer and Ribaric [29]. It consists in developing the $P_{ij}(\Theta)$ elements in the left hand sides of Eqs. (29) in series of convenient generalized Legendre functions, $P_{m,n}{}^l(\Theta)$ according to Eq. (12). The additivity theorem of these functions (see Appendix B) is such that $\cos(-m\chi + n\chi')P^l_{m,n}(\Theta)$ and $\sin(-m\chi + n\chi')P^l_{m,n}(\Theta)$ products may be expanded into Fourier series of $\cos(s(\varphi - \varphi'))$ and $\sin(s(\varphi - \varphi'))$, respectively, thus providing the required coefficients. The development is somewhat intricate. Detailed developments are given in [24,25], and a brief explanation is given in Appendix C.

After immediate rearrangements of the matrix products in Eqs. (30), with the radiance vector $\mathbf{L}^s_n$ standing for $(I^s_n, Q^s_n, U^s_n, V^s_n)^{\mathrm{T}}$ (and $\mathbf{L}^s_n = \mathbf{L}^s_{n,\cos} + \mathbf{L}^s_{n,\sin}$), identification of terms in $\cos(s(\varphi - \varphi_0))$ and $\sin(s(\varphi - \varphi_0))$ leads to the separation of Eqs. (21) into separate equations with the only variables τ and μ

$$\mathbf{L}^s_n(\tau, \mu < 0) = -\int_0^{\tau} e^{-(\tau' - \tau)/\mu} \mathbf{S}^s_n(\tau', \mu) \mathrm{d}\tau'/\mu, \tag{31a}$$

$$\mathbf{L}^s_n(\tau, \mu > 0) = \mathbf{L}^{\mathrm{up},s}_n(\tau^*, \mu > 0) e^{-(\tau^* - \tau)/\mu} + \int_{\tau}^{\tau^*} e^{-(\tau' - \tau)/\mu} \mathbf{S}^s_n(\tau', \mu)\, \mathrm{d}\tau'/\mu, \tag{31b}$$

where

$$\mathbf{S}^s_1(\tau, \mu) = \frac{\omega(\tau)}{4\pi} e^{\tau/\mu_0} \mathbf{P}^s(\tau, \mu, \mu_0)\mathbf{E}_0, \tag{31c}$$

$$\mathbf{S}^s_{n>1}(\tau, \mu) = \frac{\omega(\tau)}{2} \int_{-1}^{+1} \mathbf{P}^s(\tau, \mu, \mu')\mathbf{L}^s_{n-1}(\tau, \mu')\, \mathrm{d}\mu', \tag{31d}$$

and

$$\mathbf{L}^{\mathrm{up},s}_1(\tau^*, \mu > 0, \varphi) = (-\mu_0)\mathbf{R}^s(\mu, \mu_0)\mathbf{E}_0 e^{\tau^*/\mu_0}/\pi, \tag{31e}$$

$$\mathbf{L}^{\mathrm{up},s}_{n>1}(\tau^*, \mu > 0) = 2 \int_{-1}^{0} (-\mu')\mathbf{R}^s(\mu, \mu')\mathbf{L}^s_{n-1}(\tau^*, \mu')\, \mathrm{d}\mu' \tag{31f}$$

with $\mathbf{P}^s(\tau,\mu,\mu')$ in the form

$$\mathbf{P}^s(\tau,\mu,\mu') = \begin{pmatrix} \sum_{l=s}^{L} \beta_l P_s^l P'^l_s & \sum_{l=s}^{L} \gamma_l P_s^l R'^l_s & \sum_{l=s}^{L} -\gamma_l P_s^l T'^l_s & 0 \\ \sum_{l=s}^{L} \gamma_l R_s^l P'^l_s & \sum_{l=s}^{L} \alpha_l R_s^l R'^l_s + \zeta_l T_s^l T'^l_s & \sum_{l=s}^{L} -\alpha_l R_s^l T'^l_s - \zeta_l T_s^l R'^l_s & \sum_{l=s}^{L} \varepsilon_l T_s^l P'^l_s \\ \sum_{l=s}^{L} -\gamma_l T_s^l P'^l_s & \sum_{l=s}^{L} -\alpha_l T_s^l R'^l_s - \zeta_l R_s^l T'^l_s & \sum_{l=s}^{L} \alpha_l T_s^l T'^l_s + \zeta_l R_s^l R'^l_s & \sum_{l=s}^{L} -\varepsilon_l R_s^l P'^l_s \\ 0 & \sum_{l=s}^{L} -\varepsilon_l P_s^l T'^l_s & \sum_{l=s}^{L} \varepsilon_l P_s^l R'^l_s & \sum_{l=s}^{L} \delta_l P_s^l P'^l_s \end{pmatrix} \tag{32}$$

i.e. $\mathbf{P}^s = \mathbf{P}^s_{\cos} + \mathbf{P}^s_{\sin}$, except for the opposite sign in the upper right 4×4 sub-matrix, from the $[-\mathbf{P}^s_{\sin}\mathbf{L}^s_{n-1,\sin}]$ term in Eq. (30b).

In Eqs. (31e) and (31f), we consider that the matrix reflectance of the surface, with assumed axial symmetry, is expanded in the same form as the phase matrix, with R instead of P in Eq. (28), which leads to the same developments and rearrangements. The problem is addressed in Section 5.

In Eq. (32), the coefficients α, β, δ, γ, δ, ε, ς depend on τ according to the scattering properties of the atmosphere at level τ. The functions P_l, P_s^l, R_s^l, T_s^l are defined in Appendix B. In order to lighten the notations, with $F = P_l, P_s^l, R_s^l,$ or T_s^l, F stands for $F(\mu)$ and F' for $F(\mu')$. Note that, in the summations over l, for $l=0$ and $l=1$, only terms with β_0, β_1, δ_0 and δ_1 differ from zero. The form of $\mathbf{P}^s(\tau,\mu,\mu')$ depending of the different conventions of sign is discussed in Appendix A.

5. Surface reflectances

A major distinction has to be made between land and water surfaces. Both exhibit diffuse and specular reflectance properties but in quite inverse proportions.

Seawater surface reflects according to the well-known Fresnel's law, and the corresponding reflectance is highly anisotropic and polarizing. A realistic modeling of water surface is the model of Cox and Munk [30], which considers that the sea surface consists in a juxtaposition of wave facets, smooth enough to act like Fresnel's specular reflectors, but oriented randomly. The major resulting effect is the sunglint, localized about the specular direction, but reflection of the diffuse downward radiance is sensitive in all directions. At short wavelengths, seawater scattering leads to some diffuse water leaving radiance. In the OS code, this term is accounted for by the way of a Lambertian, i.e. isotropic and non-polarizing, reflectance.

The reflectance of land surfaces is often assumed to follow the Lambert's law. However this is only an approximation. Land reflectance is generally intermediate between that of a perfectly diffuse Lambertian reflector and that of a perfect specular reflector, which suggests it is the sum of diffuse and specular components. It is generally admitted that the diffuse component is non-polarized and emanates from multiple scattering or multiple reflection effects, while the non-diffuse component, spread about the specular direction, is polarized and emanates from single specular reflections on surface elements of the ground (leaves, rocks,...) [31,32].

Moreover, the land reflectance is much more versatile than water reflectance. Most soils have a low reflectance (5–10%) in the ultraviolet and visible spectrum, with the exception of white sand (around 40%); vegetation has also a low reflectance at short wavelengths, with a rapid increase to 30–40% in the near infrared; finally the highest reflectance is observed for snow covered ground, and can reach 90% for fresh clean snow [33].

5.1. Diffuse reflectance term

To take into account the diffuse and specular components of the reflectance, let us write $\mathbf{R}(\mu,\varphi,\mu',\varphi')$ in Eqs. (21e) and (21f) into the form

$$\mathbf{R}(\mu,\varphi,\mu',\varphi') = \mathbf{R}_{\mathrm{dif}}(\mu,\varphi,\mu',\varphi') + \mathbf{R}_{\mathrm{sp}}(\mu,\varphi,\mu',\varphi'), \tag{33}$$

where $\mathbf{R}_{\mathrm{sp}}(\mu,\varphi,\mu',\varphi')$ is examined in Section 5.2.

The non-polarized diffuse reflectance concerns only the first Stokes' parameter and leads obviously to

$$\mathbf{R}_{\mathrm{dif}}(\mu,\varphi,\mu',\varphi') = \begin{pmatrix} \rho(\mu,\varphi,\mu',\varphi') & 0 & 0 & 0 \\ 0 & 0 & 0 & 0 \\ 0 & 0 & 0 & 0 \\ 0 & 0 & 0 & 0 \end{pmatrix}. \tag{34}$$

For the Lambertian approximation, $\rho(\mu,\varphi,\mu',\varphi')$ reduces to a constant and only the azimuth independent term, $L^{s=0}$, is modified by the boundary condition.

Given some model of the land bidirectional reflectance distribution function, $\rho(\mu,\varphi,\mu',\varphi')$, symmetric about the incidence plane, generalization to anisotropic diffuse reflectance should be obtained by expanding $\rho(\mu,\varphi,\mu',\varphi')$ into the form

$$\rho(\mu,\varphi,\mu',\varphi') = \sum_{s=0}^{M}(2-\delta_{0s})\cos(s(\varphi-\varphi'))\rho^{s}(\mu,\mu') \tag{35}$$

leading to

$$\mathbf{R}^{s}_{\mathrm{dif}}(\mu,\mu') = \begin{pmatrix} \rho^{s}(\mu,\mu') & 0 & 0 & 0 \\ 0 & 0 & 0 & 0 \\ 0 & 0 & 0 & 0 \\ 0 & 0 & 0 & 0 \end{pmatrix} \tag{36}$$

in Eqs. (31e) and (31f).

5.2. Specular reflectance term

According to Cox and Munk [30], we assume that the entire water surface or some part of the land surface consists in small Fresnel's reflectors with random orientation. More precisely, let S and $\mathrm{d}S$ stand, respectively, for some horizontal area of the surface and for its fraction occupied by reflectors whose the direction of the normal is (μ_n, φ_n) within $\mathrm{d}\omega_n$. Then, the surface is characterized by the distribution function $p(\mu_n, \varphi_n)$ such that

$$p(\mu_n,\varphi_n)\mathrm{d}\omega_n = \mathrm{d}S/S. \tag{37}$$

Let us consider in these conditions the radiative flux reflected by S in direction (μ, φ) within $\mathrm{d}\omega$ when illuminated by an unpolarized parallel beam with irradiance E' in direction (μ', φ'). The flux is $\mu L^{\mathrm{up}} S\mathrm{d}\omega$, where L^{up} is the radiance reflected in direction (μ, φ). It comes from specular reflection of the incident beam on surface elements with convenient orientation (Fig. 5), which gives a flux $r(i)\mathrm{d}S_0 \cos iE'$ where $r(i)$ is the Fresnel's reflection coefficient for incident natural light; i is the incidence angle on the elements, and $\mathrm{d}S_0$ is their surface, i.e. $\mathrm{d}S/\mu_n$ or $Sp(\mu_n, \varphi_n)\mathrm{d}\omega_n/\mu_n$. According to the Snell Descartes' law, the flux within $\mathrm{d}\omega$ comes from reflectors oriented within $\mathrm{d}\omega_n$ such that $\mathrm{d}\omega = \sin(2i)2\,\mathrm{d}i\,\mathrm{d}\psi$ if $\mathrm{d}\omega_n = \sin i\,\mathrm{d}i\,\mathrm{d}\psi$ (Fig. 5). The previous expressions lead to

$$L^{\mathrm{up}} = \frac{p(\mu_n,\varphi_n)E'}{4\mu\mu_n} r(i) \tag{38}$$

that is to the bidirectionnal reflectance distribution function, say $R_{\mathrm{sp}}(i)$, such that

$$(-\mu')R_{\mathrm{sp}}(i) = \frac{\pi p(\mu_n,\varphi_n)}{4\mu\mu_n} r(i) \tag{39}$$

where μ_n, φ_n, i are derived easily from μ, φ, μ', φ'.

Generalization to polarized light is straightforward when refering the Stokes parameters to directions parallel and perpendicular to the reflection plane, which contains the normal to the elements and the incident and reflected directions. In Eq. (38), one has just to substitute to L^{up} and E' their vector forms, and to $r(i)$, the classical Fresnel's reflectance matrix $\mathbf{r}(i)$, refered to these axes, which leads to the bidirectionnal reflectance

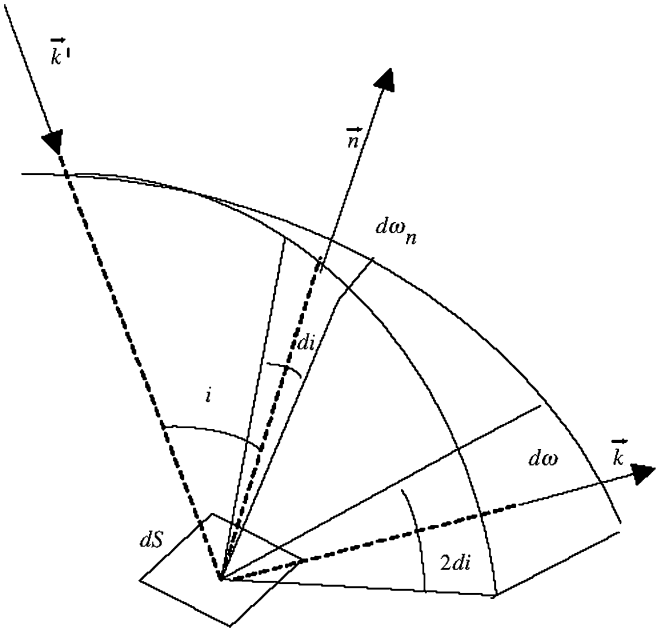

Fig. 5. The solid angle, $d\omega_n$, of normals to wave facets providing light reflected within $d\omega$, with $d\omega = 4d\omega_n$ according to the Snell–-Descartes's law.

matrix $\mathbf{R}_{sp}(i)$ such that

$$(-\mu')\mathbf{R}_{sp}(i) = \frac{\pi p(\mu_n, \varphi_n)}{4\mu\mu_n}\mathbf{r}(i) \tag{40}$$

with

$$\mathbf{r}(i) = \frac{1}{2}\begin{pmatrix} r_l^2(i) + r_r^2(i) & r_l^2(i) - r_r^2(i) & 0 & 0 \\ r_l^2(i) - r_r^2(i) & r_l^2(i) + r_r^2(i) & 0 & 0 \\ 0 & 0 & 2r_l(i)r_r(i) & 0 \\ 0 & 0 & 0 & 2r_l(i)r_r(i) \end{pmatrix} \tag{41}$$

considering for simplicity non-absorbing seawater. Generalization to complex refractive index of water is straightforward. In Eq. (41), $(r_l^2(i) + r_r^2(i))/2$ is the reflection coefficient for incident natural light, $r(i)$, introduced previously.

5.2.1. Case of land surfaces

We firstly consider the case of land surfaces. Two simple models of land surface polarization are considered in the OS code. They have been adjusted on in situ measurements of the polarized light reflected by desert surfaces and by dense vegetation covers. The models are described and compared with measurements in Breon et al [34] and in Rondeaux and Herman [35] The corresponding forms of $p(\mu_n, \varphi_n)$ are μ_n/π and $\mu_n\mu(-\mu')/[\pi(\mu-\mu')]$, respectively, which, according to Eq. (40), leads to

$$(-\mu')\mathbf{R}_{sp}(i) = h(\mu, \mu')r(i), \tag{42}$$

where

$$h_{desert}(\mu, \mu') = \frac{1}{4\mu}, \quad h_{veget.}(\mu, \mu') = \frac{(-\mu')}{4(\mu - \mu')} \tag{43}$$

for desert surfaces and vegetative covers, respectively.

Matrices $\mathbf{R}_{sp}(i)$ are refered to the reflection plane (like $\mathbf{P}(\Theta)$, Eq. (10), to the scattering plane), while Eqs. (21) need matrices $\mathbf{R}_{sp}(\mu, \varphi, \mu', \varphi')$, like $\mathbf{P}(\tau, \mu, \varphi, \mu', \varphi')$, refered to the vertical planes. As established for the scattering problem, Eq. (17) allows us to take into account the required changes in the reference axes (see Fig. 6), which gives

$$(-\mu')\mathbf{R}_{sp}(\mu, \varphi, \mu', \varphi') = h(\mu, \mu')\mathbf{T}(-\chi)r(i)\mathbf{T}(\chi'). \tag{44}$$

Given the previous expressions of $h(\mu, \mu')$, the only azimuth-dependent term in Eq. (44) is the Fresnel's matrix $\mathbf{r}(i)$, so that the expansion of $\mathbf{R}_{sp}(\mu, \varphi, \mu', \varphi')$ into Fourier series of the azimuth is straightforward when noticing the analogy of the reflection and scattering processes, with the reflection plane similar to the scattering plane, and $(\pi-2i)$ similar to the scattering angle Θ (Fig. 6). Let us develop the elements of $\mathbf{r}(i)$ in Eq. (41), in the same form as the corresponding elements of $\mathbf{P}(\Theta)$ in Eq. (12), that is, with $i = (\pi - \Theta)/2$

$$\begin{aligned}
(r_l^2(i) + r_r^2(i))/2 &= \sum_{l=0}^{P} b_l P_l(\cos\,\Theta),\\
(r_l^2(i) - r_r^2(i))/2 &= \sum_{l=2}^{P} g_l P_2^l(\cos\,\Theta),\\
(r_l^2(i) + r_r^2(i))/2 &= \sum_{l=2}^{P} [a_l R_2^l(\cos\,\Theta) + z_l T_2^l(\cos\,\Theta)],\\
r_l(i) r_r(i) &= \sum_{l=2}^{P} [z_l R_2^l(\cos\,\Theta) + a_l T_2^l(\cos\,\Theta)],\\
r_l(i) r_r(i) &= \sum_{l=0}^{P} d_l P_l(\cos\,\Theta),
\end{aligned} \tag{45}$$

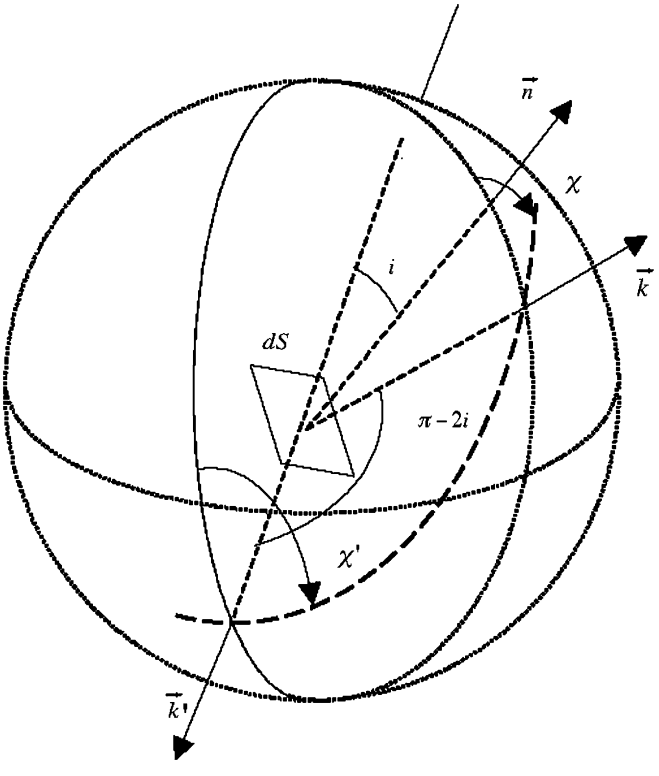

Fig. 6. The rotation angles, χ and χ', for Fresnel specular reflexion on a surface element dS.

where $\Theta = \pi - 2i$. Then, the matrix $\mathbf{T}(-\chi)\mathbf{r}(i)\mathbf{T}(\chi')$, say $\mathbf{r}(\mu, \varphi, \mu', \varphi')$, is in the form of Eqs. (28) and (29),

$$\mathbf{r}(\mu, \varphi, \mu', \varphi') = \sum_{s=0}^{M}(2 - \delta_{0s})[\cos[s(\varphi - \varphi')]\mathbf{r}^s_{\cos}(\mu, \mu') + \sin[s(\varphi - \varphi')]\mathbf{r}^s_{\sin}(\mu, \mu')] \tag{46}$$

with $\mathbf{r}^s_{\cos}(\mu, \mu')$ and $\mathbf{r}^s_{\sin}(\mu, \mu')$ derived, respectively, from $\mathbf{P}^s_{\cos}(\mu, \mu')$ and $\mathbf{P}^s_{\sin}(\mu, \mu')$ by substituting to $\alpha_l, \beta_l, \gamma_l, \delta_l, \varepsilon_l$, respectively, a_l, b_l, c_l, d_l, e_l (note that $e_l = 0$ for non-absorbing seawater).

Finally, substituting Eqs. (25) and (46) into Eqs. (21e) and (21f), the very same rearrangements and identifications as performed for the case of the source function lead obviously to expressions of $(-\mu')\mathbf{R}^s_{\mathrm{sp}}(\mu, \mu')$, in Eqs. (31e) and (31f), into the form

$$(-\mu')\mathbf{R}^s_{\mathrm{sp}}(\mu, \mu') = h(\mu, \mu')\mathbf{r}^s(\mu, \mu') \tag{47}$$

with $\mathbf{r}^s(\mu, \mu')$ in the same condensed form as $\mathbf{P}^s(\mu, \mu')$

$$\mathbf{r}^s(\mu, \mu') = \begin{pmatrix} \sum_{l=s}^{P} b_l P^l_s P'^l_s & \sum_{l=s}^{P} g_l P^l_s R'^l_s & \sum_{l=s}^{P} -g_l P^l_s T'^l_s & 0 \\ \sum_{l=s}^{P} g_l R^l_s P'^l_s & \sum_{l=s}^{P} a_l R^l_s R'^l_s + z_l T^l_s T'^l_s & \sum_{l=s}^{P} -a_l R^l_s T'^l_s - z_l T^l_s R'^l_s & \sum_{l=s}^{P} e_l T^l_s P'^l_s \\ \sum_{l=s}^{P} -g_l T^l_s P'^l_s & \sum_{l=s}^{P} -a_l T^l_s R'^l_s - z_l R^l_s T'^l_s & \sum_{l=s}^{P} a_l T^l_s T'^l_s + z_l R^l_s R'^l_s & \sum_{l=s}^{P} -e_l R^l_s P'^l_s \\ 0 & \sum_{l=s}^{P} -e_l P^l_s T'^l_s & \sum_{l=s}^{P} e_l P^l_s R'^l_s & \sum_{l=s}^{P} d_l P^l_s P'^l_s \end{pmatrix} \tag{48}$$

and with $h(\mu, \mu')$ given by Eq. (43), according to the land surface model.

5.2.2. Case of water surfaces

For the important case of the sea surface in presence of waves, the general form of the wave facet distribution function derived by Cox and Munk [30] depends on the wind direction. We restrict ourselves in the OS code to their approximate isotropic model, which depends only on the wind speed, w, and preserves the symmetry of the reflectance law. In this case

$$p(\mu_n, \varphi_n) = \frac{1}{\pi\sigma^2\mu_n^3}\exp\left(-\frac{1 - \mu_n^2}{\sigma^2\mu_n^2}\right), \tag{49}$$

where σ^2 is about $0.003 + 0.00512w$, which yields in Eq. (44)

$$h(\mu, \mu') = \frac{1}{4\sigma^2\mu\mu_n^4}\exp\left[-\frac{1 - \mu_n^2}{\sigma^2\mu_n^2}\right]. \tag{50}$$

As $h(\mu, \mu')$ also is now azimuth dependent, by the way of $\mu_n(\mu, \varphi, \mu', \varphi')$, the Fourier series development of $\mathbf{R}_{\mathrm{sp}}(\mu, \varphi, \mu', \varphi')$ needs one more step. Given w, let us develop $h(\mu, \varphi, \mu', \varphi')$ into the form

$$h(\mu, \varphi, \mu', \varphi') = \sum_{k=0}^{K}(2 - \delta_{0k})\cos(k(\varphi - \varphi'))h^k(\mu, \mu'). \tag{51}$$

Substituting Eqs. (46) and (51) into Eq. (44) gives

$$\begin{aligned}(-\mu')\mathbf{R}_{\mathrm{sp}}(\mu, \varphi, \mu', \varphi') = &\sum_{s=0}^{M}\sum_{k=0}^{K}[(2 - \delta_{0k})(2 - \delta_{0s})\cos(s\psi)\cos(k\psi)]h^k\mathbf{r}^s_{\cos} \\ &+ \sum_{s=0}^{M}\sum_{k=0}^{K}[(2 - \delta_{0k})(2 - \delta_{0s})\sin(s\psi)\cos(k\psi)]h^k\mathbf{r}^s_{\sin},\end{aligned} \tag{52}$$

where ψ stands for $(\varphi - \varphi')$, and where the (μ, μ') dependence has been omitted.

In the right-hand side of Eq. (52), multiplication by the symmetric scalar functions h^k let unchanged the structure of the matrix, so that $(-\mu')\mathbf{R}_{\rm sp}(\mu,\varphi,\mu',\varphi')$ is again in the form of Eqs. (28) and (29). Thus, writing

$$(-\mu')\mathbf{R}_{\rm sp}(\mu,\varphi,\mu',\varphi') = \sum_{s=0}^{M'}(2-\delta_{0s})[\cos[s(\varphi-\varphi')]\mathbf{r}^{*s}_{\cos}(\mu,\mu') + \sin[s(\varphi-\varphi')]\mathbf{r}^{*s}_{\sin}(\mu,\mu')] \tag{53}$$

substitution of Eqs. (25) and (53) into Eqs. (21e) and (21f) obviously leads for $(-\mu')\mathbf{R}^s_{\rm sp}(\mu,\mu')$, in Eqs. (31e) and (31f), to

$$(-\mu')\mathbf{R}^s_{\rm sp}(\mu,\mu') = \mathbf{r}^{*s}(\mu,\mu'). \tag{54}$$

In Eq. (54), $\mathbf{r}^{*s}(\mu,\mu')$ stands for the condensed form $\mathbf{r}^{*s} = \mathbf{r}^{*s}_{\cos} + \mathbf{r}^{*s}_{\sin}$, except for the opposite sign in the upper right 4×4 sub-matrix, just as $\mathbf{r}^s(\mu,\mu')$ in Eq. (47). Note that $\cos(s\psi)\cos(k\psi)$ and $\sin(s\psi)\cos(s\psi)$, in Eq. (52), provide $\cos[(s+k)\psi]$ and $\sin[(s+k)\psi]$ terms, so that $M' = M+K$, in Eq. (53).

Let us call $\mathbf{r}^{*s}_{ij}(\mu,\mu')$ the elements of $\mathbf{r}^{*s}(\mu,\mu')$, i.e.

$$\mathbf{r}^{*s}(\mu,\mu') = \begin{pmatrix} r^{*s}_{11}(\mu,\mu') & r^{*s}_{12}(\mu,\mu') & r^{*s}_{13}(\mu,\mu') & r^{*s}_{14}(\mu,\mu') \\ r^{*s}_{21}(\mu,\mu') & r^{*s}_{22}(\mu,\mu') & r^{*s}_{23}(\mu,\mu') & r^{*s}_{24}(\mu,\mu') \\ r^{*s}_{31}(\mu,\mu') & r^{*s}_{32}(\mu,\mu') & r^{*s}_{33}(\mu,\mu') & r^{*s}_{34}(\mu,\mu') \\ r^{*s}_{41}(\mu,\mu') & r^{*s}_{42}(\mu,\mu') & r^{*s}_{43}(\mu,\mu') & r^{*s}_{44}(\mu,\mu') \end{pmatrix}. \tag{55}$$

The last point is to explicit these elements in terms of the coefficients h^k and of the elements $r_{ij}{}^s$ with similar ranks i and j in Eq. (48).

Let us consider the symmetric elements, leading to the 4×4 upper left and lower right sub-matrices in Eq. (55). According to Eq. (52)

$$\sum_{0}^{M'}(2-\delta_{0s})\cos(s\psi)r^{*s}_{ij} = \sum_{l=0}^{M}\sum_{k=0}^{K}(2-\delta_{0k})(2-\delta_{0l})\cos(k\psi)\cos(l\psi)h^k r^l_{ij} \tag{56a}$$

or

$$\sum_{s=0}^{M'}(2-\delta_{0s})\cos(s\psi)r^{*s}_{ij} = \sum_{l=-M}^{M}\sum_{k=-K}^{K}\mathrm{e}^{\mathrm{i}(k+l)\psi}h^k r^l_{ij} \tag{56b}$$

assuming that $h^{-k} = h^k$ and $r^{-l}_{ij} = r^l_{ij}$. Putting $s = k+l$ (thus $k = s-l$) in Eq. (56b) and permutating the summation, with $r^{l>M}_{ij} = 0$, gives

$$\sum_{s=0}^{M'}(2-\delta_{0s})\cos(s\psi)r^{*s}_{ij} = \sum_{s=-M-K}^{M+K}\mathrm{e}^{\mathrm{i}s\psi}\sum_{l=-M}^{M}h^{s-l}r^l_{ij} \tag{56c}$$

or

$$\sum_{s=0}^{M'}(2-\delta_{0s})\cos(s\psi)r^{*s}_{ij} = h^s r^0_{ij} + \sum_{s=1}^{M+K}(2-\delta_{0s})\cos(s\psi)\sum_{l=1}^{M}[(h^{s+l} + h^{|s-l|}r^l_{ij})]. \tag{56d}$$

Identification of the terms in $\cos(s\psi)$ in Eq. (56d) thus gives

$$r^{*s}_{ij} = r^0_{ij}h^s + \sum_{l=1}^{M}r^l_{ij}(h^{l+s} + h^{|l-s|}). \tag{57}$$

Similar calculations for the anti-symmetric elements, starting from

$$\sum_{s=0}^{M'}(2-\delta_{0s})\sin(s\psi)r^{*s}_{ij} = \sum_{l=0}^{M}\sum_{k=0}^{K}(2-\delta_{0k})(2-\delta_{0l})\cos(k\psi)\sin(l\psi)h^k r^l_{ij} \tag{58}$$

but introducing now $h^{-k} = -h^k$ and $r_{ij}^{-s} = -r_{ij}^s$, lead for the elements of the 4×4 lower left and upper right sub-matrices in Eq. (55)

$$r_{ij}^{*s} = -\sum_{l=1}^{M} r_{ij}^l (h^{l+s} - h^{|l-s|}). \tag{59}$$

To sum up, Eqs. (54) and (55) provide the required boundary condition for the specular reflectance, with the elements r_{ij}^{*s} in Eq. (55) derived, according to their parity, from Eq. (57) or (59) where the coefficients h^k depend on the wind velocity and the r_{ij}^s are given by Eq. (48).

Note that an accurate development of $h(\mu, \varphi, \mu', \varphi')$ may require K as large as 96 or more. As the resulting order $M' = M + K$ of the Fourier series development of $(-\mu')\mathbf{R}_{\mathrm{sp}}^s(\mu, \mu')$, then, is generally larger than S, Eqs. (31) are applied for $s = 0, 1, \ldots, S$, and the total diffuse radiation field is given by

$$\mathbf{L}(\tau, \mu, \varphi) = \sum_{s=0}^{S} (2 - \delta_{0s})(\cos(s(\varphi - \varphi_s))\mathbf{L}^s(\tau, \mu) + \sum_{s=S+1}^{M'} (2 - \delta_{0s}) \cos(s(\varphi - \varphi_s))\mathbf{r}^{*s}(\mu, \mu_o)\mathbf{E}_s e^{\tau*/\mu_0} e^{-(\tau*-\tau)/\mu}. \tag{60}$$

The same simplification may be useful for calculations over land surfaces, when M in Eqs. (35) or (46) is larger than the useful order S (for example: $S = 2$ for pure molecular scattering).

In order to avoid the previous development of the reflectance matrix, a simplified treatment consists to consider the seawater surface as a plane horizontal water surface. Then, $\mathbf{L}_n^{\mathrm{up}}(\tau^*, \mu, \varphi)$ reduces to the specular reflection of the downward radiance $\mathbf{L}_{n-1}^{\mathrm{up}}(\tau^*, \mu', \varphi')$ in the direction $(\mu' = -\mu, \varphi' = \varphi)$. As the reflection plane coincides with the reference vertical planes, the boundary condition is simply

$$\mathbf{L}_{n>1}^{\mathrm{up}}(\tau^*, \mu > 0, \varphi) = \mathbf{r}(\theta)\mathbf{L}_{n-1}(\tau^*, -\mu, \varphi) \quad \text{for } \mu > 0, \quad \text{for } n > 1. \tag{61}$$

Eq. (61), however, stands only for $n > 1$ since the once time reflected photons are into the solar beam reflected in the specular direction $(-\mu_0, \varphi_0)$, i.e.

$$\mathbf{E}^{\mathrm{up}}(\tau) = \mathbf{r}(\pi - \theta_0)\mathbf{E}_0 e^{(2\tau^* - \tau)/\mu_0} \delta(\mu + \mu_0)\delta(\varphi - \varphi_0). \tag{62}$$

To initiate the contribution of these photons to the diffuse radiation field, primary scattering from $\mathbf{E}^{\mathrm{up}}(\tau)$ has to be taken into account into the source function $\mathbf{S}_1(\tau, \mu, \varphi)$. Accounting for this modification, after straightforward separation in azimuth, in the OS formulation of the probem, Eqs. (31c), (31e) and (31f) have to be replaced, respectively, by

$$\mathbf{S}_1^s(\tau, \mu) = \frac{\omega(\tau)}{4\pi}(e^{\tau/\mu_0}\mathbf{P}^s(\tau, \mu, \mu_0)\mathbf{E}_0 + e^{(2\tau^* - \tau)/\mu_0}\mathbf{P}^s(\tau, \mu, -\mu_0)\mathbf{r}(\pi - \theta_0)\mathbf{E}_0), \tag{63a}$$

$$\mathbf{L}_1^{\mathrm{up},s}(\tau^*, \mu > 0) = (-\mu_0)\mathbf{R}_{\mathrm{dif}}^s(\mu, \mu_0)\mathbf{E}_0 e^{\tau^*/\mu_o}/\pi, \tag{63b}$$

$$\mathbf{L}_{n>1}^{\mathrm{up},s}(\tau^*, \mu > 0) = \mathbf{r}(\theta)\mathbf{L}_{n-1}^s(\tau^*, -\mu) + \int_{-1}^{0} 2(-\mu')\mathbf{R}_{\mathrm{dif}}^s(\mu, \mu')\mathbf{L}_{n-1}^s(\tau^*, \mu')\mathrm{d}\mu'. \tag{63c}$$

6. Numerical approximations

In numerical codes, the optical depth τ and the zenith angle cosine μ are discretized, and the integrals are approximated by sums. For μ, a Gauss quadrature of even order P is chosen in Eqs. (31d) and (31f), with Gauss points μ_p, and Gauss weights a_p, which satisfy the relations $\mu_p = -\mu_{-p}$ and $a_p = a_{-p}$. For τ, the atmosphere is divided into K homogeneous layers, with interfaces at τ_k, such that $\tau_1 = 0$ and $\tau_{K+1} = \tau^*$; the layer k, of optical depth $\Delta\tau_k$, is between τ_k and τ_{k+1} (see Fig. 7).

Let us consider the upward radiance in some direction μ_p. Starting from $\mathbf{L}_1^s(\tau_{K+1}, \mu_p > 0)$ given by Eq. (31e), $\mathbf{L}_1^s(\tau_k, \mu_p > 0)$ is derived successively at levels $k = K, K-1, K-2, \ldots, 1$ from Eq. (31b)

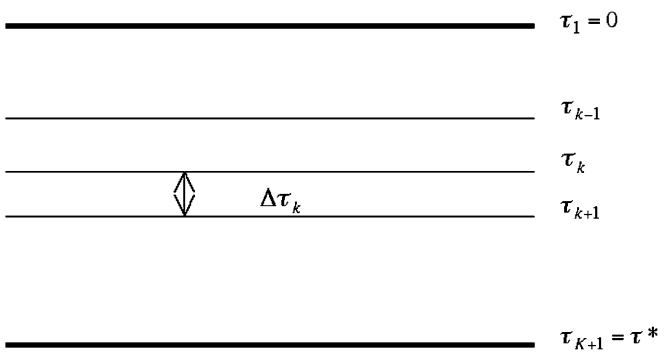

Fig. 7. Discretization of the optical depth in the atmosphere, τ.

approximated into the form

$$\mathbf{L}_1^s(\tau_k, \mu_p > 0) = \mathbf{L}_1^s(\tau_{k+1}, \mu_p > 0)e^{-\Delta\tau_k/\mu_p} + \frac{1}{4\pi}[\bar{\omega}\bar{\mathbf{P}}^s(\mu_p, \mu_0)]_k \mathbf{E}_0(e^{\tau_{k+1}/\mu_0} + e^{\tau_k/\mu_0})/2 \tag{64}$$

accounting for Eq. (31c) for $\mathbf{S}_1^s(\tau_k, \mu_p)$. The mean value of the kernel, $[\bar{\omega}\bar{\mathbf{P}}^s(\mu_p, \mu_0)]_k$, over the layer k is expressed as follows.

To handle several types of aerosols with different vertical profiles, M different modes of scattering particles may be considered, including molecules. For each mode M, the albedo, ω_m, and the phase matrix, $\mathbf{P}_m(\Theta)$, are fixed, and the total optical thickness is distributed arbitrarily between the K layers. An absorbing gas without line structure is entered as an aerosol mode, but with $\omega_m = 0$. With $\Delta\tau_{k,m}$ for the optical thickness of mode m in layer k,

$$[\bar{\omega}\bar{\mathbf{P}}^s(\mu_p, \mu_0)]_k = \left[\sum_{m=1}^{M} \omega_m \Delta\tau_{m,k} P_m^s(\mu_p, \mu_0)\right] \Bigg/ \left[\sum_{m=1}^{M} \Delta\tau_{m,k}\right]. \tag{65}$$

An equation similar to Eq. (64) stands for the primary scattering downward radiance, which is derived successively at levels $k = 2, 3, \ldots K+1$. With $\mathbf{L}_1^s(\tau_k, \mu_p)$ calculated at all levels in the 2P Gauss directions, the calculation of all $\mathbf{L}_2^s(\tau_k, \mu_p)$ is performed in the same manner, and so on. $\mathbf{L}_{n>1}^s(\tau_K, \mu_p > 0)$ is firstly derived from Eq. (31f) by a Gauss quadrature, and, accounting for the source function in Eq. (31d), for $n > 1$, Eq. (31b) is replaced by

$$\mathbf{L}_{n>1}^s(\tau_k, \mu_p > 0) = \mathbf{L}_{n>1}^s(\tau_{k+1}, \mu_p > 0)e^{-\Delta\tau_k/\mu_p} + \frac{1}{2}\sum_{q=-P}^{+P} a_q[\bar{\omega}\bar{\mathbf{P}}^s(\mu_p, \mu_q)]_k(\mathbf{L}_{n-1}^s(\tau_{k+1}, \mu_q) + \mathbf{L}_{n-1}^s(\tau_k, \mu_q))/2.s \tag{66}$$

Finally, we have to choose the order of five expansions:

- L for the phase function (or matrix) coefficients, generally given by Mie theory,
- S for the Fourier series,
- N for the number of successive scattering,
- P for the Gauss quadrature, and
- K for the number of layers.

The order L of the Mie coefficients depends on the radius r of the particles, or more precisely on the ratio $2\pi r/\lambda$ where λ is the wavelength. For Rayleigh scattering $L = 2$. For large particles L increases very fast, mainly to represent the strong forward peak. In this case, a simplification is introduced by replacing the peak with a Delta function [36]. Generally L is limited to 50 or 80.

We have seen that S is limited to $S = L$, but, in many cases, it can be much smaller, especially if the directions of interest are not too low on the horizon. When the interest is in irradiance, zenith sky radiance, or any problem with symmetry around the vertical, only $S = 0$ is needed, i.e. the azimuth independent term.

A Gauss quadrature of order P gives the exact value of the integral for a polynomial of degree smaller than or equal to $2P$. The necessary order depends on the more or less rapid angular variation of the function to be integrated. For typical terrestrial aerosols $2P = 48$ is convenient.

The number N of scattering to use for a precision ΔL on the radiance, is in principle such that $(\tau^*)^N \approx \Delta L$, but the convergence is generally tested in the code. Moreover, the ratio L_{n+1}/L_n tends to become constant for large n, allowing to approximate the high orders of scattering by a geometrical series.

For moderate solar zenith angles and optical thicknesses (say $\tau^* \approx 0.1 - 0.5$), K between 20 and 30 is reasonable. For an expected accuracy $\Delta L \approx 10^{-4}$, $K \approx 100$ is needed.

7. Examples of applications of the OS code

The OS code described above is multifunctional and flexible, and it can be used for various purposes. In order to clarify the possible applications, let us first summarize the input parameters to the code and its outputs.

The major input parameters are:

(i) the atmospheric profiles of air molecules, absorbing molecules, and various types of aerosols,
(ii) the properties (function of wavelength) of the atmospheric constituents, extinction coefficient, single scattering albedo, phase matrix for all scatterers, absorption cross sections for absorbing gases,
(iii) the surface reflectance characteristics, and
(iv) the solar zenith angle.

We have seen in Section 6 that the orders of 5 expansions have to be chosen, i.e. L for the phase function or matrix, S for the Fourier series, N for the number of successive scatterings, P for the Gauss quadrature, K for the number of layers. Assuming that these orders are correctly chosen, the result accuracy depends only on the accuracy of the input parameters.

A final parameter is the radiation wavelength, which has to be fixed at the beginning of the code. Most generally the code includes a loop over wavelengths in a given spectral interval; the choice of wavelengths can be either discrete, for analyzing data obtained with filter instruments, or continuous, with a fixed step, when analyzing spectral measurements.

The direct outputs of the code are:

(i) the radiance $L(\tau, \mu, \varphi)$ at directions (μ, φ), and at levels τ either defined by the discretizations, or requested by the user. The output radiance is proportionnal to the input value for E_0. By entering $E_0 = 1$, the output is given in unit of the extraterrestrial solar flux E_0; then, if the radiance is wanted in energetic units, the code output has to be multiplied by the extraterrestrial flux [37]. By entering $E_0 = \pi$, the output is given in unit of dimensionless normalized radiance, $\pi L/E_0$ and
(ii) the two Stokes parameters $Q(\tau, \mu, \varphi)$ and $U(\tau, \mu, \varphi)$ for the same level and directions; $V(\tau, \mu, \varphi)$ is very small and generally neglected. The degree of polarization and its direction are derived from Eqs. (6)–(8).

From the radiance, important integral quantities can be derived: (i) the upward and downward irradiances received on an horizontal plane; their difference is the net flux which determines the radiative heating rate; (ii) the upward and downward spherical (or actinic) fluxes; their sum is the total actinic flux, in which the radiance from each direction has the same weight; the total actinic flux determines the photochemical reactions in the atmosphere These integral quantities depend only on the azimuth independent term of the radiance; moreover, the influence of polarization is, in this case, negligible. Therefore they can be obtained by a simplified version of the code.

As mentioned above, the results can be obtained at any level τ in the atmosphere. But the levels of interest are most often, either the surface ($\tau = \tau^*$), for analysis of ground-based observations, or the top of the atmosphere ($\tau = 0$), for analysis of satellite observations. This corresponds to the two main applications developed at LOA. One of them concerns the analysis of remote sensing of aerosols: the code is run for a few

discrete wavelengths, corresponding to the instrument channels, and the output data are radiance and polarization at the top of the atmosphere, for the satellite observation directions. The other concerns the analysis of ultraviolet (UV) spectral observations at the Earth's surface, the code is run with a narrow step over wavelength in the ultraviolet range, and ozone absorption is included; the useful output data are the irradiance and/or the actinic flux at the surface.

A few other cases have been considered, and the code has been made available to other research groups. Let us mention, as examples:

- computations of visible sky radiance, for validation purpose with various atmospheric models [38] and
- distribution of sky radiance at two UV wavelengths taking into account molecular polarization [39].

7.1. Remote sensing

Applications of the code are described in papers concerning atmospheric modeling for the Earth observation from the top of the atmosphere (TOA) (e.g. [40]) and aerosol remote sensing from ground-based measurements (e.g.[41]). More recently, in the context of the POLDER experiment [42], the code was used for the vicarious calibration of the system [43] and for aerosol retrievals over land surfaces (e.g. [44]) and over the ocean (e.g. [45]).

Examples of the code outputs are shown in Figs. 8–10. Figs. 8 and 9 illustrate the problem of the sea surface modeling for aerosol retrieval over the ocean. To estimate the range of the sunglint contamination in TOA

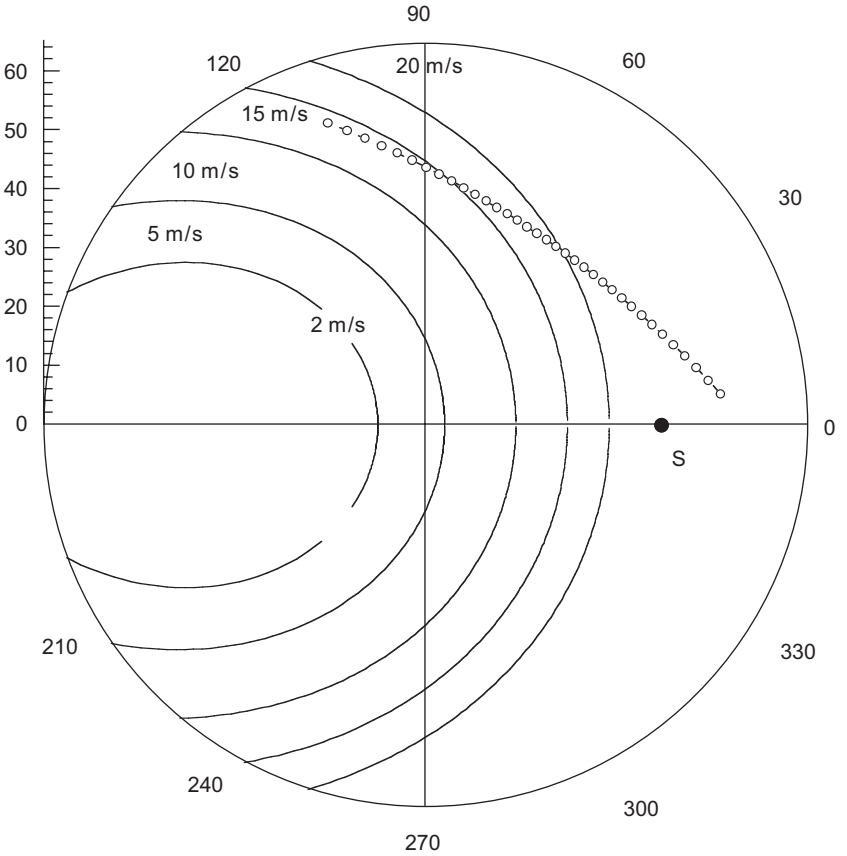

Fig. 8. Polar plot of viewing directions, (θ, φ), at TOA. The solar zenith angle is 40° (S). Continuous curves correspond to normalized radiance of the sunglint equal to 0.001, according to the model of Cox and Munk, for wind speeds ranging from 2 to 20 m/s. Circles show observation geometries, convenient for aerosol observations, for which measurements are simulated in following Figs. 9 and 10.

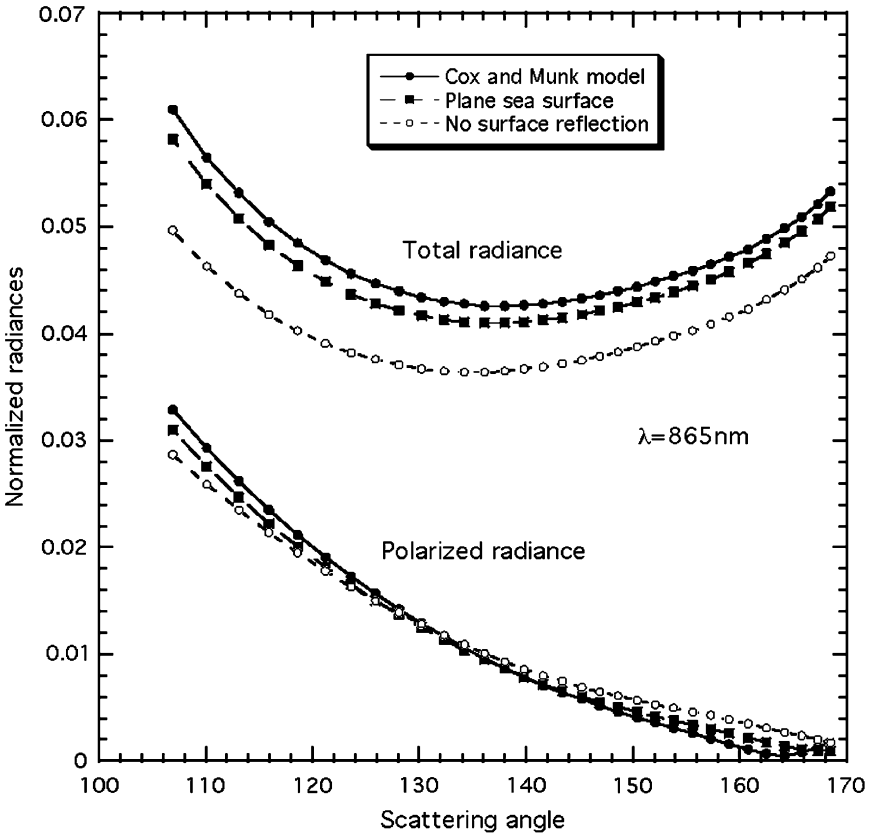

Fig. 9. Influence of the sea surface modeling in TOA measurements. For the viewing geometries given by circles in Fig. 8 and the aerosol model described in the text, the radiance (upper curves) and polarized radiance (lower curves) at TOA are reported as a function of the scattering angle with, respectively, reflection on the sea surface neglected (circles), accounted for by the plane sea surface approximation (squares), and accounted for by the Cox and Munk isotropic model for $w = 7$ m/s (dots). The radiances are normalized, which means that the extraterrestrial flux E_0 is taken equal to π.

observations, the continuous curves in Fig. 8 show, in polar coordinates (θ, φ), viewing directions for which the sunglint normalized radiance, $\pi L(\theta, \varphi)/E_0$, is 0.001, according to the Cox and Munk isotropic model, for wind speeds ranging from 2 to 20 m/s. Circles are examples of viewing directions reasonably preserved from the sunglint, convenient for aerosol observations. The corresponding scattering angles range about from 105° to 170°.

For these viewing geometries, Fig. 9 shows, as a function of the scattering angle, the normalized total radiance and polarized radiance derived from the code for $\lambda = 865$ nm, for an aerosol optical thickness $\tau^* = 0.25$. The aerosol consists in a fine mode of spherical particles with real refractive index $m = 1.45$; the size distribution is log-normal, with modal radius $\bar{r} = 0.08\,\mu$m and variance $\sigma = 0.46$, as described in [45]. The assumed wind speed is 7 m/s. and the ocean-backscattered radiation is assumed to be zero. For comparison, the results obtained using the approximation of plane sea surface and neglecting the surface effect (i.e. only the atmospheric contribution) have been also reported. As seen in Fig. 9, complete modeling of the sea surface effect is worthwhile.

Fig. 10 illustrates the influence of the aerosol vertical profile. As Fig. 9, it presents the normalized total and polarized radiances, in function of the scattering angle, but for different aerosol profiles. For the same conditions as in Fig. 9, molecules and aerosols are mixed with vertical density profiles in the form $\exp[-z/H]$ and $\exp[-((z - z_0)/\Delta z)^2]$, respectively, with $H = 8$ km and $\Delta z = 0.75$ km. The TOA radiances calculated for $z_0 = 2$, 8 and 16 km are nearly the same for $\lambda = 865$ nm and are not presented, but, for $\lambda = 443$ nm, Fig. 10 shows that the measurements are sensitive to the altitude of the aerosol layer, especially the polarized light.

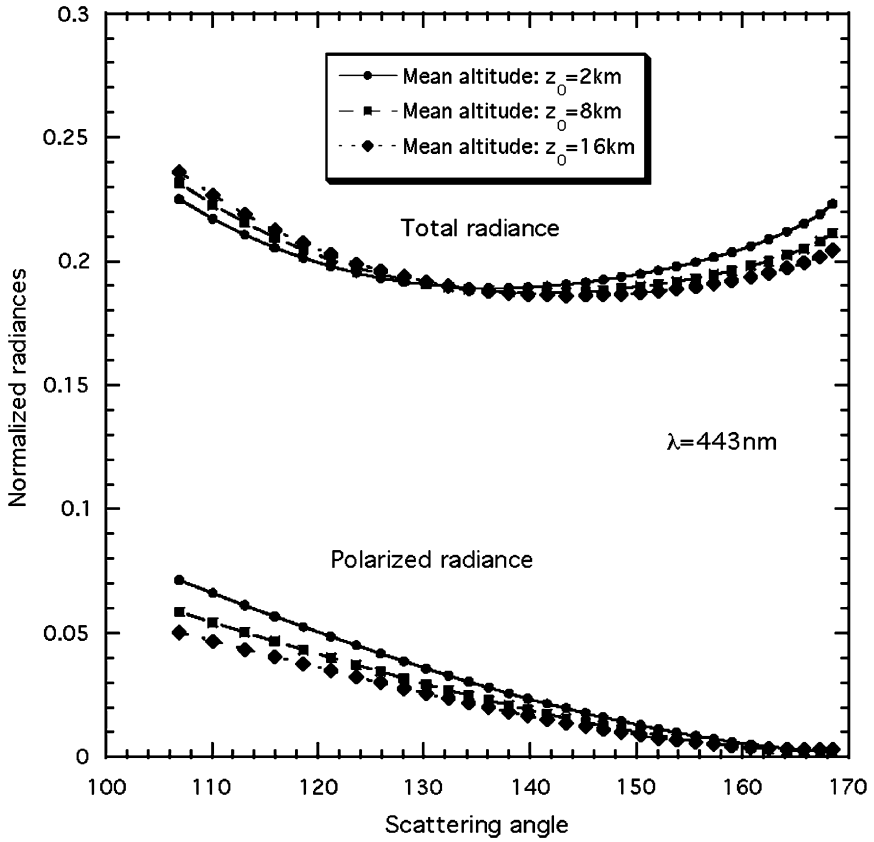

Fig. 10. Influence of the aerosol vertical profile in TOA measurements at short wavelengths. Normalized radiance (upper curves) and normalized polarized radiance (lower curves), for the same aerosol model as in Fig. 9, but for $\lambda = 443$ nm, and for 3 mean altitudes z_0 (see text) of the aerosol layer.

Because of the extinction effect of the aerosols, the lack of the molecular contribution to polarized light becomes sensitive at shorter wavelengths.

7.2. Spectral UV irradiance

This particular version of the OS code has been developed for analyzing the influence of the various atmospheric parameters on the spectral UV irradiance, observed at several ground-based stations in Europe, including two French stations, at Villeneuve d'Ascq and at Briançon. This activity was part of two successive programmes of the European Commission, SUVDAMA (Scientific UV Data Management) and EDUCE (European Database for Ultraviolet Radiation Climatology and Evaluation), and of a third one, CUVRA (Characteristics of UV Radiation field in the Alps), more specifically devoted to the Alpine regions.

The code is run from 280 to 450 nm, with a wavelength step of 0.5 nm at wavelengths shorter than 345 nm, in order to follow the small oscillations of the ozone absorption cross section; at larger wavelengths the step is 5 nm. We have checked that the influence of polarization on irradiance is negligible, because of a compensation between the different directions. Only the azimuth independent part of radiance is computed. For the sun lower than 30° above the horizon, the pseudo-spherical approximation is used. In order to have absolute values to compare to measurements, the irradiance given by the code for $E_0 = 1$, is first interpolated to 0.05 nm, which is the resolution of the best UV extra terrestrial spectrum [46]; after multiplication by the extraterrestrial flux, the irradiance (now in $\mathrm{W\,m^{-2}\,nm^{-1}}$) is convoluted with the instrument slit function (around 0.5 nm).

The results have been compared to measurements, in case of very low turbidity [47], where the uncertainty on aerosol amount and characteristics, has an almost negligible impact. The results of several different codes have also been intercompared [48] for different atmospheres.

Successive reflectances between a highly reflecting snow-covered ground and the sky backscattering lead to a strong enhancement of the diffuse irradiance. This enhancement has been analyzed theoretically with the OS code [49]; for fresh clean snow and clear sky, it could reach about 50% at its maximum, around 320–330 nm. The problem is made more complex, because the snow cover is generally non-homogeneous. At Briançon site, the snow enhancement has been analyzed during the winter 2002, and the maximum enhancement found to be about 25%. This is conveniently expressed in term of an effective albedo [50], which would lead for an homogeneous reflecting surface, to the same enhancement observed for the inhomogeneous actual surface.

The same code has also been used successfully, to compute the actinic flux during an international intercomparison of models and measurements, performed in Boulder, June 1998 [51].

8. Conclusion

In this paper, we have presented a radiative code, based on the successive orders of scatterings, developed at LOA. The code uses the vector form of the radiative transfer equation, which takes into account polarization effects. The code in its complete form, can handle different aerosol models, and Earth's surface reflection laws. The different discretizations used in the code, have been carefully tested, and the accuracy of the results depends only on the accuracy of the input parameters.

We have given up the idea of proposing one more ''monster code'', which can be used as a black box, for solving any problem, at the cost of unnecessary long computer time, and of a large risk of error. The code can be obtained in different versions from the authors, and the detailed description given in this paper, aims at helping the potential users to make their own choice between versions, and to adapt the code at best to their own problem.

Acknowledgements

This study was funded by the 'Centre National d'Etudes Spatiales' (CNES), the 'Centre National de la Recherche Scientifique' (CNRS), the European Commission, the 'Conseil Régional du Nord-Pas de Calais', the 'Fonds Européen de Développement Régional', and the 'Délégation Régionale à la Recherche et à la Technologie du Nord-Pas de Calais'. The authors would like to acknowledge Christine Deroo and Louis Gonzalez for computational help.

Appendix A. Symmetries and sign rules

As outlined by Van der Mee and Hovenier [24], the final vector form of the problem depends on the employed conventions.

Given the coefficients $(\alpha_l, \beta_l, \ldots, \varepsilon_l)$ and $(a_l, b_l, \ldots, e_l)$ and the incident solar irradiance, the numerical solution of the ET depends only on the structures of $\mathbf{P}(\tau, \mu, \varphi, \mu', \varphi')$ and $\mathbf{R}(\mu, \varphi, \mu', \varphi')$. They have been obtained here assuming that $(\mathbf{l}, \mathbf{r}, \mathbf{k})$ is a right-handed cartesien coordinate system, and that φ and χ are counted in the direct direction, respectively, around Oz and $\mathbf{k}$.

Let us count the azimuth in the opposite direction. The same radiation field then gives opposite signs of the numerical values of U and V according to Eq. (24). Obviously, this is obtained by changing the signs of the elements anti-symmetric with respect to $(\varphi - \varphi')$ in $\mathbf{P}^s(\tau, \mu, \mu')$ and $\mathbf{R}^s(\mu, \mu')$, i.e. the upper right and lower left 4×4 submatrices. In the mathematical development, this change comes from the $P^l_{m,n}(\Theta)$ addition theorem, with opposite sign for the $\sin(-m\chi + n\chi')P^l_{m,n}(\cos\Theta)$ development when using opposite direction for the azimuth (Appendix B, Eq. (B.8)).

Going back to the usual sign for φ let us use $(\mathbf{r}, \mathbf{l}, \mathbf{k})$ rather than $(\mathbf{l}, \mathbf{r}, \mathbf{k})$ as a right-handed coordinate system, with $\mathbf{r}$ in the opposite direction for example. The phase retardation of E_l relative to E_r, δ, is changed into $\delta + \pi$, and the same radiation field gives again opposite numerical values of U and V (Eq. (5)), which leads to the

same changes in $\mathbf{P}^s(\tau,\mu,\mu')$ and $\mathbf{R}^s(\mu,\mu')$. In the mathematical development, the change comes now from opposite signs of the sinus terms in the rotation matrix $\mathbf{T}(\chi)$, with χ unchanged but with opposite signs for E_r and E'_r.

Finally, the equations are unsensitive to χ since changing the positive direction for rotation around $\mathbf{k}$ leads to change both the form of the rotation matrix and the sign of the $\sin(-m\chi+n\chi')P^l_{m,n}(\cos\Theta)$ development, so that both changes compensate. Of course, equations are unchanged when changing both the azimuth positive direction and the right-handed coordinate system, which leads to two formulations only of the ET.

Appendix B. Generalized Legendre functions

We use here generalized Legendre functions, which derive from the functions introduced by Gel'fand and Sapiro, refered to as GS [26], by

$$P^l_{m,n}(\mu) = (i)^{m-n} P^l_{m,n}(\mu)_{\mathrm{GS}}, \tag{B.1}$$

where the subscript [GS] designs the original functions. Therefore our functions are real, and their definition, derived from GS definition, is

$$P^l_{m,n}(\mu) = A^l_{m,n}(1-\mu)^{(m-n)/2}(1+\mu)^{-(m+n)/2}\frac{d^{l-n}}{d\mu^{l-n}}((1-\mu)^{l-m}(1+\mu)^{1+m}), \tag{B.2}$$

$$A^l_{m,n} = \frac{(-1)^{l-m}}{2^l(l-m)!}\sqrt{\frac{(l-m)!(l+n)!}{(l+m)!(l-n)!}}, \tag{B.3}$$

where l, m, n are integers; m and n can be positive, negative or zero; l is $\geqslant \sup(|m|,|n|)$. The $P^l_{m,n}(\mu)$ satisfy the normalization

$$\int_{-1}^{+1} P^l_{m,n}(\mu)P^{l'}_{m,n}(\mu)\mathrm{d}\mu = \delta_{ll'}\frac{2}{2l+1}. \tag{B.4}$$

Other important relations, derived from GS, are

$$P^l_{-m,n}(\mu) = (-1)^{l-n}P^l_{m,n}(-\mu), \tag{B.5a}$$

$$P^l_{m,n}(\mu) = P^l_{-n,-m}(\mu) = (-1)^{m-n}P^l_{n,m}(\mu) = (-1)^{m-n}P^l_{-m,-n}(\mu). \tag{B.5b}$$

$P^l_{0,0}(\mu)$ reduces to the Legendre polynomial $P_l(\mu)$, and $P^l_{m,0}(\mu)$ to the usual associated Legendre function $P^l_m(\mu)$.

Addition theorem

In its general form, it reads as

$$e^{-\mathrm{i}m\chi}P^l_{m,n}(\cos\Theta)e^{\mathrm{i}n\chi'} = (-1)^n\sum_{s=-l}^{l}(-1)^s e^{\mathrm{i}s(\varphi-\varphi')}\{P^l_{m,s}(\mu)P^l_{s,n}(\mu')\}, \tag{B.6}$$

which gives

$$\cos(-m\chi+n\chi')P^l_{m,n}(\cos\Theta)=P^l_m(\mu)P^l_n(\mu')+\sum_{s=1}^{l}\cos[s(\varphi-\varphi')]\{P^l_{s,m}(\mu)P^l_{s,n}(\mu')+P^l_{s,-m}(\mu)P^l_{s,-n}(\mu')\}, \tag{B.7}$$

$$\sin(-m\chi+n\chi')P^l_{m,n}(\cos\Theta)=\sum_{s=1}^{l}\sin[s(\varphi-\varphi')]\{P^l_{s,m}(\mu)P^l_{s,n}(\mu')-P^l_{s,-m}(\mu)P^l_{s,-n}(\mu')\}. \tag{B.8}$$

Recurence relations

The general recurence relation

$$\begin{aligned}&l\sqrt{(l+1)^2-m^2}\sqrt{(l+1)^2-n^2}P^{l+1}_{m,n}(\mu)+(l+1)\sqrt{l^2-m^2}\sqrt{l^2-n^2}P^{l-1}_{m,n}(\mu)\\&\quad=(2l+1)(l(l+1)\mu-mn)P^l_{m,n}(\mu)\end{aligned} \tag{B.9}$$

reduces to the usual recurences for the Legendre polynomials and for the Legendre associated functions. The derived recurence relations for the $R^l_s(\mu)$ and $T^l_s(\mu)$ functions defined in Eqs. (13) are

$$\begin{aligned}&l\sqrt{(l+1)^2-s^2}\sqrt{(l+1)^2-4}R^{l+1}_s(\mu)+(l+1)\sqrt{l^2-s^2}\sqrt{l^2-4}R^{l-1}_s(\mu)\\&\quad=(2l+1)\big(l(l+1)\mu R^l_s(\mu)-2sT^l_s(\mu)\big),\end{aligned} \tag{B.10a}$$

$$\begin{aligned}&l\sqrt{(l+1)^2-s^2}\sqrt{(l+1)^2-4}T^{l+1}_s(\mu)+(l+1)\sqrt{l^2-s^2}\sqrt{l^2-4}T^{l-1}_s(\mu)\\&\quad=(2l+1)\big(l(l+1)\mu T^l_s(\mu)-2sR^l_s(\mu)\big)\end{aligned} \tag{B.10b}$$

with

$$R^2_0(\mu)=\sqrt{3/8}(1-\mu^2),\quad T^2_0(\mu)=0,\ T^{l>2}_0(\mu)=0, \tag{B.11a}$$

$$R^2_1(\mu)=-\mu\sqrt{1-\mu^2}/2,\quad T^2_1(\mu)=-\sqrt{1-\mu^2}/2, \tag{B.11b}$$

$$R^2_2(\mu)=(1+\mu)^2/4,\quad T^2_2(\mu)=\mu/2 \tag{B.11c}$$

and for $s\geqslant 2$

$$R^s_s(\mu)=\frac{1}{2^s}(1+\mu^2)(1-\mu^2)^{s/2-1}\sqrt{\frac{(2s)!}{(s+2)!(s-2)!}}, \tag{B.11d}$$

$$T^s_s(\mu)=\frac{1}{2^s}2\mu(1-\mu^2)^{s/2-1}\sqrt{\frac{(2s)!}{(s+2)!(s-2)!}}. \tag{B.11e}$$

Appendix C. Expression of the coefficients $(\mathbf{P}^s(\tau,\mu,\mu'))_{ij}$

The expansion of the kernel matrix $\mathbf{P}(\mu,\varphi,\mu',\varphi')$, into Fourier series has been first obtained by Kuscer and Ribaric [29], using a representation of the electric field on two inverse circular vibrations, instead of two linear vibrations, as done for the Stokes parameters. After some intricate mathematics, it is possible to deduce the expansions with Stokes parameters by combining the Kuscer and Ribaric expansions. We have chosen here to start directly with the expansions obtained for the elements $P_{ij}(\Theta)$ (Eqs. (12)). Let us consider $\mathbf{P}(\mu,\varphi,\mu',\varphi')$ in Eq. (27).

The terms P_{11} and P_{44}, according to Eq. (12), are simply expanded into a series of Legendre polynomials. The usual additivity theorem of the Legendre polynomials leads to the expressions in Eq. (32). This is easy to understand, remembering that P_{11} is identical to the phase function p.

The eight other terms of the first and last columns and rows , after introducing Eqs. (12), contain the functions P^l_2 $(\cos\Theta)$, multiplied by $\cos(2\chi)$ or $\sin(2\chi)$, or by the same functions of χ'. Using Eqs. (B.7) and (B.8), written for $(m=0,\ n=2)$ and $(m=2,\ n=0)$, with the definitions in Eqs. (13), the expressions in Eq. (32) are easily obtained.

The four central terms of $\mathbf{P}(\mu,\varphi,\mu',\varphi')$ are somewhat more difficult to obtain, and we will give some hints about the method to use.

In order to make appear terms with $\cos(-m\chi+n\chi')$ and $\sin(-m\chi+n\chi')$, let us introduce

$$u(\Theta)=(P_{22}(\Theta)+P_{33}(\Theta))/2, \tag{C.1}$$

$$v(\Theta)=(P_{22}(\Theta)-P_{33}(\Theta))/2 \tag{C.2}$$

which transforms the first term into

$$cc'P_{22}+ss'P_{33}=\cos(-2\chi+2\chi')u(\Theta)+\cos(2\chi+2\chi')v(\Theta); \tag{C.3}$$

similar expressions are obtained for the three other terms.

Let us write Eqs. ((B.7) and (B.8) for $(m=-2$ and $n=2)$ and for $(m=2$ and $n=2)$ and introduce again the functions $R^l_s(\mu)$ and $T^l_s(\mu)$. With some rearrangement, it comes four equations, like

$$\cos(-2\chi+2\chi')P^l_{2,2}(\cos\,\Theta)=\sum_{s=0}^{l}(2-\delta_{0,s})\cos(s(\varphi-\varphi'))[R^l_s(\mu)R^l_s(\mu')+T^l_s(\mu)T^l_s(\mu')]. \tag{C.4}$$

Then, let us develop $u(\Theta)$ and $v(\Theta)$ into the form

$$u(\Theta)=\sum_{l=2}^{L}\eta_l P^l_{2,2}(\cos\,\Theta), \tag{C.5}$$

$$v(\Theta)=\sum_{l=2}^{L}\xi_l P^l_{-2,2}(\cos\,\Theta). \tag{C.6}$$

Substituting Eq. (C.4) and the three similar equations with Eqs. (C.5) and (C.6) into the four equations similar to Eq. (C.3) yields Fourier series developments of the central terms.

With

$$\alpha_l=\eta_l+\xi_l, \tag{C.7}$$

$$\varsigma_l=\eta_l-\xi_l \tag{C.8}$$

the expressions in Eq. (32) are found.

References

[1] Lenoble J, editor. Radiative transfer in scattering and absorbing atmospheres: standard computational procedures. A. Deepak Publishing; 1985 300pp.

[2] Mayer B, Kylling A. Technical note: The libRadtran software package for radiative transfer calculations—description and examples of use. Atmos Chem Phys 2005;5:1855–77 Available at http://www.libradtran.org.

[3] Stamnes K, Tsay SC, Wiscombe W, Jayaweera K. A numerical stable algorithm for discrete-ordinate-method radiative transfer in multiple scattering and emitting layered media. Appl Opt 1988;27:2502–9.

[4] Madronich S. The TUV software package. ⟨ftp://acd.ucar.edu/user/sasha⟩.

[5] De Haan JF, Bosma BP, Hovenier JW. The adding method for multiple scattering calculations of polarized light. Astron Astrophys 1987;183:371–97.

[6] Evans KF, Stephens GL. A new polarized atmospheric radiative transfer model. JQSRT 1991;46:413–23.

[7] Lyapustin AI. Radiative transfer code SHARM for atmospheric and terrestrial applications. Appl Opt 2005;44:7764–72.

[8] Cahalan RF, et al. The I3RC. Bringing together the most advanced radiative transfer tools for cloudy atmospheres. BAMS 2005;86:1275–93.
[9] Postyliakov OV, Belikov YuE, Nikolaishvili ShS, Rozanov A. A comparison of radiation transfer algorithms for modeling of the zenith sky radiance observations used for the determination of stratospheric trace gases and aerosols. In: Smith WL, Timofeyev YM, editors. IRS 2000: current problems in atmospheric radiation. A. Deepak Publishing, 2001 p. 885–8.
[10] Loughman RP, Griffioen E, Oikarinen L, Postylyakov OV, Rozanov A, Flittner DE, et al. Comparison of radiative transfer models for limb-viewing scattered sunlight measurements. J Geophys Res 2004;109:D06303.
[11] Chandrasekhar S. Radiative transfer. Oxford University Press, 1950. Dover Publications; 1960. 393pp.
[12] Van de Hulst HC. Multiple light scattering. Tables, formulas, and applications, 2 volumes. New York: Academic Press; 1980 739pp.
[13] Liou KN. Radiation and cloud processes in the atmosphere. Oxford: Oxford University Press; 1992 487pp.
[14] Lenoble J. Atmospheric radiative transfer. A. Deepak Publishing; 1993 532pp.
[15] Mishchenko MI, Travis LD, Lacis AA. Radiative transfer and coherent backscattering. Cambridge: Cambridge University Press; 2006 478pp.
[16] Lacis AA, Chowdhary J, Mishchenko MI, Cairns B. Modeling errors in diffuse-sky radiation: vector vs. scalar treatment. Geophys Res L 1998;25:135–8.
[17] Stokes GG. Trans Camb Philos 1852;9:399.
[18] Hovenier JW. A unified treatment of polarized light emerging from a homogeneous plane-parallel atmosphere. Astron Astrophys 1987;183:363–70.
[19] Mie G. Beiträge zur optik trüber medien, speziell kolloidaler metallösungen. Ann Phys 1908;25:377–445.
[20] Hansen JE, Travis LD. Light scattering in planetary atmospheres. Space Sci Rev 1974;16:527–610.
[21] Mishchenko MI, Hovenier JW, Travis LD, editors. Light scattering by non spherical particles. New York: Academic Press; 2000 690pp.
[22] Volten H, Munoz O, Rol E, de Haan JF, Vassen W, Hovenier JW. Scattering matrices of mineral aerosol particles at 441.6 and 632.8 nm. J Geophys Res 2001;106:17,375–401.
[23] Deuzé JL, Herman M, Santer R. Fourier series expansion of the transfer equation in the ocean–atmosphere system. JQSRT 1989;41:483–94.
[24] Van der Mee CVM, Hovenier JW. Expansion coefficients in polarized light transfer. Astron Astrophys 1990;228:559–68.
[25] Siewert CE. On the phase matrix basic to the scattering of polarized light. Astron Astrophys 1982;195–200.
[26] Gel'fand IM, Sapiro ZY. Representation of the group of rotations of 3-dimensional space and their applications. Am Math Transl 1956;2:207–316.
[27] Hammad A, Chapman S. The primary and secondary scattering of sunlight in a plane stratified atmosphere of uniform composition. Philos Mag 1939;28:99.
[28] Min Q, Duan M. A successive order of scattering model for solving vector radiative transfer in the atmosphere. JQSRT 2004;87:243–59.
[29] Kuscer I, Ribaric M. Matrix formalism in the theory of diffusion of light. Opt Acta 1959;6:42–51.
[30] Cox C, Munk W. Measurements of the roughness of the sea surface from photographs of the Sun's glitter. J Opt Soc Am 1954;44:836–50.
[31] Coulson KL, Bouricius GM, Gray EL. Optical reflection properties of natural surfaces. J Geophys Res 1965;70:4601–11.
[32] Vanderbilt VC, Grant L. Plant canopy specular reflectance model. IEEE Trans Geosci Remote Sens 1985;GE-23:722–30.
[33] Warren SG, Wiscombe WJ. A model for the spectral albedo of snow.I: pure snow. J Atmos Sci 1980;37:2712–33.
[34] Bréon FM, Tanré D, Lecomte P, Herman M. Polarized reflectance of bare soils and vegetation; measurements and models. IEEE Trans Geosci Remote Sens 1995;33(2):497–9.
[35] Rondeaux G, Herman M. Polarization of light reflected by crop canopies. Remote Sens Environ 1991;38:63–75.
[36] Wiscombe WJ. The Delta-M method: rapid yet accurate radiative flux calculations for strongly asymmetric phase functions. J Atmos Sci 1977;34:1408–22.
[37] Available on SORCE site: 〈http://lasp.colorado.edu/sorce/〉.
[38] Sherlock V, Hauchecorne A, Lenoble J. Methodology for the independent calibration of Raman backscatter water–vapor lidar calibration. Appl Opt 1999;38:5816–37.
[39] Huber M, Blumthaler M, Screder J, Schallhart B, Lenoble J. Effect of inhomogeneous surface albedo on diffuse UV sky radiance at a high-altitude site. J Geophys Res 2004;109:D08107.
[40] Tanré D, Herman M, Deschamps PY, de Leffe A. Atmospheric modeling for space measurements of ground reflectances, including bidirectional properties. Appl Opt 1979;18:3587–94.
[41] Devaux C, Vermeulen A, Deuzé JL, Herman M, Santer R, Verbrugghe C. Retrieval of aerosol single-scattering albedo of from ground-based measurements. Application to observational data. J Geophys Res 1998;103(D8):8753–61.
[42] Deschamps PY, Bréon FM, Leroy M, Podaire A, Bricaud A, Buriez JC, et al. The POLDER mission: instrument characteristics and scientific objectives. IEEE Trans Geosci Remote Sens 1994;32:598–615.
[43] Hagolle O, Goloub P, Deschamps PY, Cosnefroy H, Briottet X, Bailleul T, et al. Results of POLDER in-flight calibration. IEEE Trans Geosci Remote Sens 1999;37:1550–66.
[44] Deuzé JL, Bréon FM, Devaux C, Goloub P, Herman M, Lafrance B, et al. Remote sensing of aerosols over land surfaces from POLDER-ADEOS1 polarized measurements. J Geophys Res 2001;106(D5):4913–26.
[45] Herman M, Deuzé JL, Marchand A, Roger B, Lallart P. Aerosol remote sensing from POLDER/ADEOS over the ocean: improved retrieval using a nonspherical particle model. J Geophys Res 2005;110:D10S02.

[46] Van Hoosier ME. The ATLAS-3 solar spectrum, available via anonymous ftp (ftp://susim.nrl.navy.mil./pub/atlas3), 1996.
[47] Pachart E, Lenoble J, Brogniez C, Masserot M, Bocquet JL. Consistency tests on UV spectral irradiance measurements using modeling and a broadband instrument. J Geophys Res 2000;105:4851–6.
[48] Van Wiele M, et al. From model intercomparison toward benchmark UV spectra for six real atmospheric cases. J Geophys Res 2000; 105:4915–25.
[49] Lenoble J. Modeling of the influence of snow reflectance on ultraviolet irradiance for cloudless sky. Appl Opt 1998;37:2441–7.
[50] Lenoble J, Kyling A, Smolskaia I. Impact of snow cover and topography on ultraviolet irradiance at the Alpine station of Briançon. J Geophys Res 2004;109:D16209.
[51] Bais AF, et al. International photolysis frequency measurement and model intercomparison (IPMMI): Spectral actinic solar flux measurements and modeling. J Geophys Res 2003;108(D16):8543.